Surface temperature condition monitoring methods for aerospace turbomachinery: exploring the use of ultrasonic guided waves

To cite this article before publication: Lawrence Yule *et al* 2021 *Meas. Sci. Technol.* in press https://doi.org/10.1088/1361-6501/abda96

Abstract

Turbine blades and nozzle guide vanes (NGVs) are operated at extreme temperatures in order to maximise thermal efficiency and power output of an engine. In this paper the suitability of existing temperature monitoring systems for turbine blades and nozzle guide vanes are reviewed. Both offline and online methods are presented and their advantages and disadvantages are examined. The use of offline systems is well established but their online equivalents are difficult to implement because of the limited access to components. There is the need for an improved sensor that is capable of measuring temperature in real time with minimum interference to the operating conditions of the engine, allowing operating temperatures to be increased to the limits of the components and maximising efficiency. Acoustic monitoring techniques are already used for a large number of structural health monitoring (SHM) applications and have the potential to be adapted for use in temperature monitoring for turbine blades and NGVs. High temperatures severely affect the response of ultrasonic transducers. However, waveguides and buffer rods can be used to distance transducers from extreme conditions, while piezoelectric materials such as YCOB and AlN have been developed for use at high temperatures. A new monitoring approach based on ultrasonic guided waves is introduced in this paper. The geometry of turbine blades and NGVs allows Lamb waves to propagate through their structure, and the presence of numerous cooling holes will produce acoustic reflections that can be utilised for monitoring temperature at a number of locations. The dispersive nature of Lamb waves makes their analysis difficult; however, wave velocity in dispersive regions is particularly sensitive to changes in temperature and could be utilised for monitoring purposes. The proposed method has the potential to provide high resolution and accuracy, fast response times, and the ability to place sensors outside of the gas path. Further research is required to develop a monitoring system based on the use of guided waves in extreme environments.

Surface temperature condition monitoring methods for aerospace turbomachinery: exploring the use of ultrasonic guided waves

Lawrence Yule, Bahareh Zaghari, Nicholas Harris, Martyn Hill

December 17, 2020

1 Introduction

This review considers recent surface temperature monitoring methods for turbomachinery applications, focusing on jet engine turbine blades and nozzle guide vanes (NGVs). Monitoring of these parts is important for a number of reasons: identifying potential failures before they occur, evaluating the need for maintenance, investigating ways of improving engine efficiency, and reducing fuel consumption.

Carbon dioxide emission is the largest contributor from aviation to global warming, comprising 70% of aircraft engine emissions [1]. A small improvement in the design of a jet engine will result in a sizable reduction in pollution, as well as in fuel and engine costs [2, 3]. The results of temperature monitoring can inform the research and development process to improve the operation and efficiency of components [4]. More accurate monitoring in terms of absolute temperature, spatial resolution, and time history allows for further development, maximising the effectiveness of components. Current and past methods focus on testing parts in controlled environments before installation in an engine, with the majority of methods requiring the blade or vane to be removed from the engine for analysis after a test has taken place. This can be improved with online methods that allow for monitoring during normal engine operation. Online methods provide considerably more data for analysis during start-up and cool down of the engine rather than only providing a peak result. The currently available online methods can only provide point measurements (in the form of thermocouples) or require optical access (pyrometry & thermographic phosphors) which is difficult to achieve in the cramped conditions of a turbine. These online systems have been utilised in test rigs and gas turbines but have not been adapted for use on in-service jet engines because of space, weight, and power constraints. An improvement to these sensors would greatly benefit gas turbine manufacturers, allowing for further development in turbine blade and NGV design by better understanding their limits. If the uncertainty of temperature measurements can be reduced then engine efficiency can be improved by operating components closer to their ideal conditions [5].

An increase in turbine inlet temperature elevates the risk of blade failure from blade creep or oxidation, the extent to which is determined by the exposure time at raised temperatures [6]. Blades and vanes require constant cooling with film cooling techniques embedded into their structure to avoid corrosion and melting [7], with gas temperatures up to 1000°C using uncooled blades and around 1800°C with cooled blades [8]. The air used for film cooling is drawn from the main gas path, reducing efficiency while increasing NO_X emissions [9]. As emission limits become stricter the use of film cooling may have to be reduced, emphasising the importance of temperature monitoring to allow components to be operated closer to their thermal limits. Components such as turbine blades and NGVs are coated with ceramic based thermal barrier coatings (TBCs) to allow gas stream temperatures to be further increased. These coatings are normally multilayered, utilising yttrium-stabilised-zirconia (YSZ; Y_2O_3–ZrO_2) as the insulating material, a thermally grown oxide layer

(TGO), and a bonding layer to attach to the substrate [10]. The most likely point of failure from exposure to excessively high temperatures [11] is considered to be at or near the TBC/TGO interface, which makes monitoring of this area vital for maintaining blade health. Reviews of condition monitoring/non-destructive evaluation (NDE)/structural health monitoring (SHM) for all aspects of gas turbines are provided by Abdelrhman [12] and Mevissen [13], however there are a limited number of studies that focus on developments in online surface temperature monitoring for jet engines, which is covered in the first half of this paper.

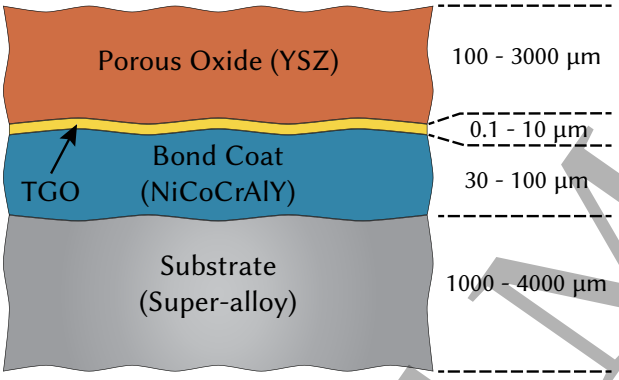

Figure 1: Cross section of a typical turbine blade with TBC applied [14].

Acoustic methods are a potential alternative that have already been utilised for a number of other SHM and NDE applications. Ultrasonic guided waves in particular offer many benefits including low costs, high accuracy, and fast response times if utilised correctly. Acoustic waves transmitted through the structure of a blade or vane would not interfere with their operation, and temperature measurement at multiple locations could be achieved by utilising the acoustic reflections from the large number of cooling holes found across the structure. The difficulties of this method are in managing the impact of high temperatures on electronic components [15] and sensor operation, which requires appropriate material selection and signal processing techniques. There are a number of different options for the generation and acquisition of waves, methods of coupling to the structure, and temperature derivation, all of which need to be investigated further to determine the most suitable method. The second half of this paper discusses the potential of acoustic methods and how they can be implemented for use on turbine blades and NGVs.

In the next section the methods currently used for temperature monitoring of turbine blades and NGVs are discussed. Starting with numerical simulations used in the design stage, followed by offline systems used for validation, and finally online systems used in monitoring engines during normal operation. The monitoring of rotating turbine blades differs from that of static nozzle guide vanes, which is discussed for each monitoring method. Summaries of the methods can be found in tables 1 and 2. The following section discusses an alternative temperature monitoring system that aims to address the limitations of the current methods, based on the use of ultrasonic guided waves. The most suitable methods of attaching sensors to the structure of a blade or vane are discussed, followed by an explanation of how Lamb waves can be utilised for this application.

2 Current surface temperature monitoring strategies

Numerical simulations are used in the design stage of blades and vanes to predict the efficiency of cooling techniques before parts are put into production. Experimental data from offline or online monitoring can then be compared to numerical simulations for validation. Offline systems record the peak temperatures of the blade for later analysis at room temperature while online measurements are carried out in real time. The majority of the offline systems are well established having been used for many years, with online systems being more difficult to implement and operate reliably as sensors need to be installed inside of the engine. The implementation of online systems is further complicated when applied to jet engines, as there are severe restrictions on space, weight, and power. The systems can be further categorised into either point measurement methods or mapping meth-

ods, where point-based systems only record the temperature at a single location, but can be installed in arrays to provide more spatial information. Mapping methods allow for continuous measurement across the surface of the blade, allowing for analysis of temperature gradients.

2.1 Numerical methods for temperature estimation

Numerical simulations are used to find the cooling effectiveness of turbine blades and NGVs. Results of the simulations are validated against experimental results, such as those from temperature-sensitive paints [16]. Finite element modelling (FEM) can be used to predict the thermal load on a blade and analyse the effectiveness of blade cooling methods. There are two methods of calculations, uncoupled or coupled. Uncoupled methods are less computational intensive as the heat transfer coefficients used in the calculations are only computed at key engine operating conditions. Coupled methods use computational fluid dynamic (CFD) calculations to iterate the heat transfer coefficients, which improves accuracy over uncoupled methods. Findeisen *et al.* [17] compared two coupled methods, FEM1D and FEM2D. The FEM1D method uses simplified models of the cooling system making it suitable for initial designs, while the FEM2D method uses three dimensional CFD simulations that are more realistic but nearly a hundred times slower than FEM1D. This makes FEM2D models more suitable for comparison with experimental data. In order to validate complex thermal models over 80% of the surface should be measured, which is not possible with point measurement systems such as thermocouples [18]. Thermal maps allow manufacturers to better understand the effects of air flow on specific areas of components, which can help to improve the life cycle of a part. Areas of increased thermal stress can be identified, which may require additional cooling or design adjustment, while also highlighting less critical areas that could be reduced in weight or cooling.

2.2 Offline Monitoring Methods

Offline monitoring methods rely on an irreversible physical change to occur in order to accurately record the peak temperature of a surface. A summary of the available offline methods is shown in table 1. Thermal paints and thermal history sensors are the most commonly used methods as they allow temperature to be mapped across the surface of the blade or vane while being less intrusive than other methods.

2.2.1 Thermal paint or Temperature indicating paint (TIP)

Specially formulated paints can be applied to the surface of a blade or vane that irreversibly change colour after exposure to high temperatures, recording the peak temperature at which they were exposed. Irreversible thermochromism takes place because of decomposition, i.e. changes to the crystal structure because of chemical reactions that produce new compounds. The change in colour is both a function of temperature and time, requiring careful control of exposure time for accurate analysis. Yang *et al.* [19] describe the development of temperature indicating paints including their formulation, application, and test methodology. Paints can be categorised as single-change or multi-change, whereby single-change paints change colour once after exceeding a particular temperature threshold, and multi-change paints undergo multiple colour changes as temperature increases past a number of thresholds. Multi-change paints are more suitable for use on parts with large temperature gradients, such as turbine blades or NGVs. Examples of commercially available thermal paints produced by Thermographic Measurements Ltd, UK, can be seen in figures 2 and 3 [20]. Results can be visually interpreted by an operator drawing isothermal lines, or analysed with automated image processing techniques. When analysis is carried out by an operator only a small number of temperature changes can be identified, where colour changes are obvious. In order to measure a greater range of temperature changes other blades can be monitored with different paints during the same test. Results from the different blades can then be combined to provide

Method	Temperature range (°C)	Temperature resolution (°C)	Spatial resolution	Sensor type	Interrogation method
Crystal temperature sensors	up to 1400	+/-10	Low	Surface mounted	Illumination + observation
Templugs	650	15-25	Low (single points)	Embedded in substrate	Analysis of ferromagnetism/hardness/phase
Glass ceramic arrays	1100	Not given	Low	Surface mounted	Observation only
Temperature sensitive paints (TIP)	Up to 1500	10-100	Moderate	Surface layer	Observation only
Thermal history paint (THP)	150-1400	+/-5	High	Surface layer or embedded in TBC	Illumination + observation

Table 1: Summary of offline temperature monitoring methods

a more detailed map. When analysis is carried out using image processing techniques accuracy can be improved to identify colour changes representing ±10°C changes, however inconsistent lighting conditions can cause significant sources of error. A large range of different paints can be used, covering the temperature range 150°C-1300°C. This range can be further extended to 1500°C with the use of fluorescent paint that is analysed under UV rather than visible light [21], which reduces the chance of operator error and the effect of variable lighting conditions [22]. Engine test data is often used to validate numerical models. In order to produce quantitative results from the use of thermal paints, the engine test data must be compared with calibration data, without which the paints only provide qualitative spatial information. Laboratory-based tests can be carried out to replicate engine conditions while the temperature is monitored using other methods (e.g. thermocouples, IR cameras) for validation of the real engine data. Another option is to validate the real data using predictions based on the paint's chemistry [23]. Colour changes are cross sensitive to environmental gases which must be accounted for when comparing results to calibration charts. Low paint durability means that testing time should be limited to between 3 and 5 minutes at peak temperatures for best results. [24]. Longer exposure time makes it difficult to determine if a colour change has occurred due to peak temperatures over a short period or lower temperatures over a longer period. Dismantling the engine for analysis can be time consuming and additional tests require the paint to be removed and reapplied before the engine is reconstructed. Many thermal paints contain cobalt, nickel, or lead compounds that are restricted for use by EU legislation (REACH [25]) because of their toxicity.

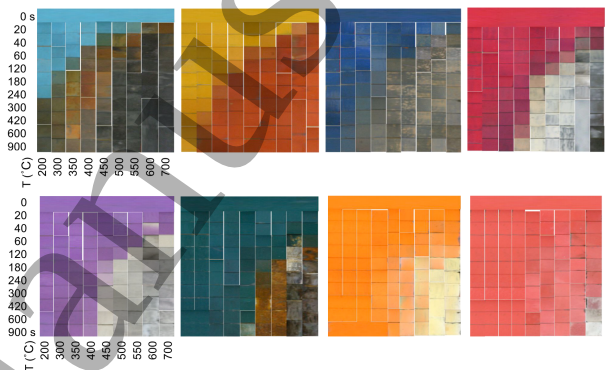

Figure 2: Time at temperature colour maps for single-change paints: SC155, SC240, SC275, SC367, SC400, SC458, SC550, SC630 [20].

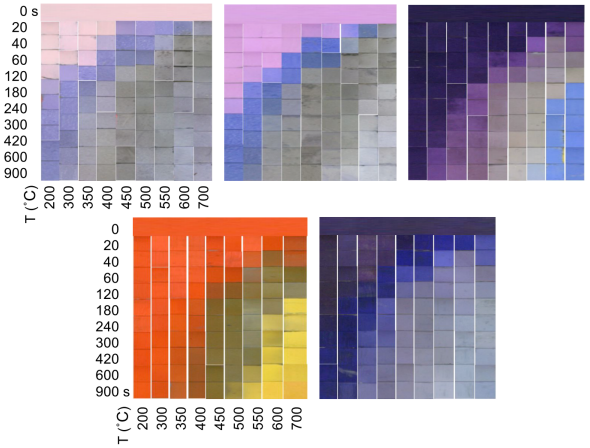

Figure 3: Time at temperature colour maps for multi-change paints: MC135-2, MC165-2, MC395-3, MC490-10, MC520-7 [20].

2.2.2 Thermal history paint (THP)

Thermal history paints are based on ceramic materials doped with luminescent transition or rare-earth ions. They are similar in principle to thermal paints/temperature indicating paints in that exposure to high temperatures causes irreversible changes to their optical properties. When subjected to high temperatures the detection material transforms from the amorphous state to the crystalline state, which results in a change in the luminescence properties, including the luminescence spectrum and the lifetime decay. This transformation depends on thermal history, which includes the temperature to which the component has been subjected, and the time at that temperature. The method was originally proposed by Feist in 2007 [26]. Resolution and accuracy is improved in comparison to thermal paints/temperature indicating paints as the optical change is continuous across the surface of the part and can be analysed with an emission detector, as with online thermographic phosphors. Parts do not have to be fully dismantled for analysis, and the phosphors do not contain restricted chemicals (EU REACH regulation [25]). Biswas and Feist [27] discuss the theoretical background of thermal history sensors, their analysis methods, and carry out an experimental comparison against thermal paints and thermocouples. Results show good agreement between thermal paints/temperature indicating paints and thermal history paints from 400°C to 900°C. Standard deviation of the thermal history coating measurement is typically below 5°C. Peral *et al.* [18] has developed an uncertainty model for the use of thermal history sensors from 400°C to 750°C, indicating that the maximum estimated uncertainty was ±6.3°C or ±13°C for 67% or 95% confidence levels respectively. This is believed to be well within the uncertainty of thermal models and the requirements for temperature measurements in harsh environments on gas turbines.

Araguas Rodriguez *et al.* [28] have carried out temperature measurements between 350°C and 900°C on three types of NGVs (without cooling, internally cooled, externally cooled) and compared the results to an embedded thermocouple. The THP was made up of an oxide ceramic pigment mixed into a water-based binder doped with lanthanide ions. Measurements are carried out using a handheld probe, each taking approximately five seconds. Precision of the measurement was ±5°C, and results were within the min-max range of the thermocouple results. An extended test (around 50 hours) using THPs was carried out by Pilgrim [29]. No damage to the THP was observed, and results are in agreement with temperature sensitive paints and CFD models (10°C difference between them). This shows an improvement over temperature sensitive paints, which can only be used for short term (∼5 minutes) engine tests. The processes behind the optical changes that are caused by temperature are explained by Rabhiou *et al.* [30], followed by experimental results that show a Y_2SiO_5:Tb phosphor suitable for use up to 1000°C, with potential for further development to extend the upper temperature limit to 1400°C. A resolution comparison between thermal paints/temperature indicating paints, pyrometry, and thermal history sensors is given by Amiel [31] in Table 2. Pyrometry methods provide the highest resolution (0.3°C), followed by thermal history sensors (1-5°C), and finally temperature sensitive paints (10-100°C). Heyes [32] carried out tests using a Y_2SiO_5:Tb phosphor suspended in a binder that could be used for temperature measurement from 400°C to 900°C. Results showed that the use of the binder caused some signal degradation, inhibiting the crystallisation process of the phosphor. This indicated the potential benefits of integrating the phosphors into TBCs, which negates the need for a binder. A preliminary investigation was carried out utilising air plasma spraying (APS) of YAG:YSZ:Dy which showed promising results.

Although accuracy and resolution are improved in comparison to thermal paints, optical access to the parts is still required for analysis, which requires dismantling of the engine but not the parts themselves. Paints need to be removed and reapplied to carry out additional tests. The application of the paints requires sophisticated coating technologies which limits their uses. Careful phosphor selection is required as emission intensity decreases with increasing temperatures [11].

2.2.3 Other offline sensors

A number of other offline sensors have been developed for use on turbine blades or vanes that are described below. The use of these sensors is limited in comparison to temperature sensitive paints or thermal history sensors as they only provide point measurements while being more intrusive to blade operation.

Crystal temperature sensors have been developed to more accurately measure temperature gradients across blades in comparison with thermal paint methods. A crystal structure is installed on surface of the blade using thermo-cement and exposed to neutron radiation ("illumination"), causing the atomic lattice to expand. When exposed to heat the lattice relaxes, which can be analysed with an X-ray diffraction microscope. If exposure time is also measured the temperature can be deduced from comparison with a calibration diagram. Accuracy of the method is ±10°C, up to at least 1400°C [33].

Glass ceramic arrays rely on using materials that all undergo different allotropic phase transformations when exposed to temperature changes. Using a single material will result in the same phase change whether the material is exposed to a high temperature for a short time, or a low temperature for a long time, which can be accounted for when using a number of materials. As temperature and exposure time increases optical transmittance is reduced, which can be measured using a UV light spectrophotometer. A disadvantage of this method is that it is strongly influenced by moisture in the environment (as found in aircraft engine exhausts), which causes large changes in the crystallisation structure of the glass. It also suffers from an inability to account for overheat events unless they are of sufficient magnitude (>50°C) [34].

Metallurgical temperature sensors are a family of offline sensors that can be machined into almost any shape. They are best suited to applications where wire connections are not possible, especially those where the sensor is immersed in a corrosive medium. Their accuracy is poor in comparison to thermocouples (around 10°C) and they can only be used to give rough estimates of temperature. Stainless steel "Feroplugs" reduce in ferromagnetism with increasing temperature exposure, which can be measured using a ferritscope or magnetic suspectometer. The reduction in ferromagnetism fully diminishes above 600°C, the upper limit of temperature measurement. Sigmaplugs have been developed to extend the measurement range, introducing a new phase that can be measured up to 900°C. Templugs are made of steel alloys that reduce in hardness with increasing temperature. The change in hardness can be measured and compared with calibration charts to determine the temperature if exposure time is known. Accuracy is around 15°C up to 600°C, reducing to 25°C up to 650°C [35]. Madison *et al.* [36] compared metallurgical temperature sensors with thermocouples when measuring piston temperatures in a running engine. Results were comparable however the metallurgical sensors were heavily influenced by areas with large thermal gradients.

2.3 Online Monitoring Methods

Online methods are used to measure temperature in real-time. This is particularly useful in comparison to offline methods as the monitoring can take place at start-up and cool down of the engine, rather than only providing a peak result. Accurate measurement of the peak exposure temperature requires separation of time and temperature effects, which is not necessary for online methods. Another benefit over offline methods is the reduction in research and development time as the engine does not need to be dismantled between each test, which in turn reduces cost. This enables in-service data collection as opposed to short-term engine test data gathered from offline monitoring. Additional data helps to further validate numerical models when online systems are installed in test rigs, but they can also be used for condition monitoring applications on in-service engines. More comprehensive monitoring is beneficial in reducing maintenance schedules as these can be based on component health rather than a fixed number of operational hours. This has the benefits of reducing maintenance costs whilst minimising downtime. A reduction in the frequency of blade replacement is also beneficial to the environment. Table 2 shows the currently available online monitoring methods. For ro-

tating turbine blades pyrometry based methods are commonly used as they do not require a phosphor coating or laser excitation to operate (as with thermographic phosphors), and scanning methods can be used to monitor a whole row of blades with single sensor system. They are also less intrusive than point-based thermocouple or resistance temperature detector (RTD) arrays, which require complex telemetry systems to transmit the sensor signals outside of the engine. Thermographic phosphors are utilised in scenarios where pyrometry issues cannot be mitigated, and can be used to calibrate/correct pyrometer measurements [37]. For static nozzle guide vanes pyrometry cannot be used to scan the surface and so an array of thermocouples are typically used.

2.3.1 Thermocouples

Conventional thermocouples are not suitable for use on turbine blades or NGVs, as their large size disrupts airflow, and reliably attaching them to the surface of a blade is difficult. Thin film thermocouples (TFTC) on the other hand can be directly fabricated on to the surface of a turbine blade or NGV, greatly improving long term durability in comparison to conventional thermocouples. COMSOL simulations carried out by Duan *et al.* [38] show a ~170°C difference between conventional thermocouples and their thin-film counterparts due to the distance between the thermocouple joint and the blade surface. The placement of a conventional thermocouple in its insulation filling adds an additional uncertainty of around 500 × 500 µm, which has a temperature difference from top to bottom of ~300°C. The uncertainty associated with the use of conventional thermocouples shows the motivation for the development of thin film equivalents.

The small footprint of TFTCs does not affect airflow, leading to more accurate measurements of fast temperature fluctuations. TFTCs have an extremely fast response time (<1 µs), are low cost, and have very fine spatial resolution at a single point. S-type platinum plus platinum 10% rhodium thermocouples have been shown to be stable up to 1100°C. However, oxidation of rhodium (which would occur in the gas path of a turbine) causes the thermoelectric potential to decrease, which in turn limits the upper working temperature of these types of thermocouple [39]. The main challenges to overcome with TFTCs are: developing an electrical insulation film that can withstand the harsh conditions of the turbine (high temperatures, shock, and vibration), and applying the sensor to curved surfaces.

Yang *et al.* [40] have shown that an S-type thermocouple can be fabricated using pulsed laser deposition (PLD) techniques that functions up to 700°C. To improve thermal stability at high temperatures composite ceramic oxides can be used, which have good anti-oxidation properties and have been shown to maintain high thermal outputs up to 1200°C [41]. Direct-Write Thermal Spray (DWTS) is a process by which powder, wire, or rods can be adhered to a complex substrate such as a blade or vane. A thermocouple can be embedded into the TBC on the surface of an NGV in this way and has been shown to perform well up to 450°C [42]. The addition of Al_2O_3 to YSZ(yttria-stabilized zirconia)-based TBCs improves their electrical insulation above 400°C which allows TFTCs to be used effectively [43]. A summary of THTC systems is given by Satish *et al.* [44] along with the implementation of a K-type TFTC on an NGV deposited using an E-beam evaporation technique. Two methods of measuring temperature distribution on a TBC coating are given by Z. Ji *et al.* [45] whereby Pt soldering dots are placed along a PtRH thin film. Measurements are possible up to 1200°C with this method.

Despite the improvement of thin film thermocouples over conventional thermocouples they are still an invasive monitoring method. Only point measurements are possible unless installed in dense arrays which can have an impact on blade operation, requiring complex wiring systems. The connection between thin-film and leadwires is the primary failure point when installed on turbine blades, and complex telemetry systems are required to transmit sensor signals outside of the engine [46]. Oxidation has a significant impact on the operation of TFTCs at high temperatures, causing drift and delamination [47], which makes the use of an insulation material vital.

Method	Temperature range	Temperature resolution (°C)	Spatial resolution (°C)	Sensor type	Interrogation method
Thin film thermocouples (TFTCs)	Up to 1200	+/-2	Low (can be installed in arrays)	Surface mounted	Electrical connection
Infrared Thermography/Pyrometry	500->2000	0.3	Low (blades can be scanned)	Optical probe	Observation only
Temperature sensitive paints (MLCs)	<200	1-5	High	Surface layer	Illumination + observation
Thermographic phosphors	Up to 1600	1-5	High	Surface layer or embedded in TBC	Illumination + observation

Table 2: Summary of online temperature monitoring methods

2.3.2 Pyrometry

Optical pyrometry is a non-contact method of measuring thermal radiation emitted from the surface of a material. There is no upper temperature limit as thermal radiation increases with temperature, but there is a lower limit of around 500°C [48]. Measurement response is fast in comparison to conventional thermocouples as there is no thermal inertia to overcome. In order to implement a pyrometry system in a turbine optical access is required, which can be achieved by routing a probe through the wall of the turbine casing and connecting it to a detector via fibre optic cable, away from the high temperature environment of the turbine [48]. The system can be considered a point measurement system for nozzle guide vanes as the probe is focused on an area 1-10 mm in diameter, however the point can be scanned across the surface of turbine blades to produce temperature maps [49]. A review of fibre optic thermometry methods is given by Yu *et al.* [50], covering blackbody, infrared, and fluorescence optical thermometers. For accurate results the emittance of the blades must be measured prior to installation to later be used in correcting the output of the pyrometer, however the emittance is also affected by factors such as surface roughness, oxidation state, and chemical composition, which will affect the overall accuracy of the system. A number of solutions have been proposed to improve the accuracy of emittence measurement, namely dual and triple wavelength pyrometry [5, 51]. A review of multi-spectral pyrometry systems is given by Araújo *et al.* [52]. Accuracy is also affected by reflected radiation from other surfaces within the turbine, absorption of radiation in the gas path, interference from hot particles, and deposits forming on the surface of the probe lens. The effectiveness of short wavelength (∼1 microns) pyrometry is negatively affected by the application of TBCs, which reduces emittance while increasing reflectivity of the blades. The optical transparency of TBCs causes significant measurement errors [53], while the thermal gradient of TBCs (∼0.5°C/µm) means that careful wavelength selection is required to ensure that measurement is taking place at the required depth [54]. Long wavelength (∼10 microns) pyrometry has been developed to overcome this problem, where TBC emittance is reliably close to 1, and reflectance is close to 0. Long wavelengths are non–penetrating [55] and have been shown to work effectively during engine tests [56], although the readings are strongly influenced by background radiation. A number of authors have tested pyrometers on turbine engine test rigs [6, 57, 58]. Taniguchi *et al.* [59] have carried out temperature measurements using a pyrometer on a turbine blade rotating at 14,000 RPM. The system has a measurement range of 700-1150°C with an accuracy of ±3°C, over a 2 mm diameter area. The measurement probe is only inserted into the hot section of the engine for a short time (10s) before being removed to avoid damage, which limits the long term use of this method. To avoid placing the sensor into the turbine during measurement (which can cause gas disturbances), multiple beam pyrometry methods have been developed [60, 61]. Infrared thermography has also been used on gas turbines for crack and defect detection rather than absolute temperature measurement [62]. Although pyrometry can provide high accuracy (in favourable conditions) and fast response times, the need for optical access and their large size restricts their uses to dedicated test rigs and large gas turbines. It is unlikely that a pyrometry system could be installed inside of a jet engine for SHM applications without considerable reductions in size and weight. During long term use the build up of deposits on the surface of the probe lens will reduce accuracy and require regular mainte-

nance. In order to produce temperature maps of nozzle guide vanes the probe must be scanned across the surface which would require mechanical movement of the probe, a potential point of failure.

2.3.3 Temperature sensitive paints

Temperature sensitive paints (TSPs) differ from thermal paints or temperature indicating paints in that they do not undergo permanent changes to their structure after exposure to high temperatures. The temperature dependence of luminescent molecules can be measured after application to the surface of a material using a polymer binder. The luminophore is excited by a light source, causing thermal quenching to take place. The intensity or decay lifetime of the luminescence can be measured using a camera, both of which are temperature dependent [63]. A selection of TSPs are described by Patel *et al.* [64], showing their useful temperature ranges. At low temperatures (<200°C) metal-ligand complexes (MLCs) are used as luminophores, whereas at high temperature thermographic phosphors are used.

2.3.4 Thermographic phosphors

Thermographic phosphors can be used in a very similar way to the metal-ligand complexes (MLCs) used in temperature sensitive paints however they are suitable for use up to much higher temperatures (∼1600°C). They can be excited and analysed in the same way as TSPs using laser excitation and fluorescence detectors. A number of authors have carried out reviews of thermographic phosphor systems, covering the principles and theory of fluorescence [65], instrumentation [66], implementation [67], and discussion of phosphor materials and error analysis [68]. Phosphors can be applied to a blade or vane in a number of ways, the simplest of which is to mix the phosphor with a binder and apply it to the surface of the TBC, which provides a surface temperature measurement. A phosphor layer can also be applied beneath the TBC, which allows for monitoring of the temperature critical bonding layer. This is difficult to achieve as YSZ is mostly opaque to UV radiation, making excitation of the phosphor a challenge [14]. Phosphors can also be directly integrated into TBCs, acting as thermal insulation and as a sensor simultaneously. The first investigation into using phosphors embedded into TBCs, called 'smart coating' or 'thermal barrier sensor coating' was carried out by Feist [11]. Further development has shown that the addition of phosphors to produce sensor coatings does not affect the structure of TBCs and they can be applied using the same air plasma spray (APS) process as non-doped TBCs [69]. The system has been applied to an NGV in a Rolls-Royce Viper 201 engine with optical access provided through a dedicated window [70]. A comparison between temperature measurements from a TBC doped sensor, pyrometer, and thermocouple shows a large temperature gradient between the surface of the TBC and the surface of the substrate, with the phosphor sensing taking place close to the bond coat interface [37].

Online temperature measurements from 513°C to 767°C have been carried out on an operating engine by Jenkins *et al.* [71]. Measurements were carried out at rotational speeds up to 32,750 RPM. A laser was used for excitation of two phosphors applied to the TBC of the turbine blades, while a fibre optic probe was used for detection. Results were found to be within 25°C of of those estimated by the engine manufacturer. It is suggested that measurement range (from engine off to maximum engine power) can be improved by utilising Y_2O_3:Er phosphors [72]. Nau *et al.* [73] have presented results from the use of five different phosphors that allow measurements from room temperature up to 1500°C. Comparison of the phosphors show that their individual temperature ranges are limited (400°C). Measurements were carried out on two model combustor systems, and at high pressure, to demonstrate the potential application in real turbines. Measurements are demonstrated with a high speed camera, allowing for temporal resolution up to 1 kHz.

The main limitation of using thermographic phosphors is the need for optical access, both for excitation and detection, which is normally achieved with fibre optic probes. Careful selection of phosphor material is required to cover the entire temperature range of interest and to ensure that emission intensity is high enough for accurate detection at ele-

vated temperatures [11]. In the case of turbine blades the excitation and detection needs to be synchronised with blade rotation which requires extremely fast response times [54], and is limited by the decay rate of the phosphor.

2.3.5 Other methods

Duan *et al.* [74] have found that the electrically conductive nature of TBCs at elevated temperatures (above 600°C) can be utilised as a form of smart sensor, by measuring a change in resistance with temperature. Experimental data shows good repeatability up to 950°C, measurement error of less than 3%, fast response time (∼1s), and stability comparable to conventional thermocouples and TFTCs.

3 Emerging techniques for online monitoring

The ideal sensor for jet engine turbine blade and NGV temperature monitoring should be capable of mapping the temperature of a blade or vane in real time with minimum interference to operating conditions. The use of a sensor should not reduce the lifetime of the blade, cause damage to its structure, require large amounts of power, or require regular maintenance, ideally surviving for the lifetime of the engine. Response time should be fast in order to accurately record the changes in temperature during start-up, shut-down, and overshoot events, while resolution and accuracy should be comparable to traditional monitoring methods.

Ultrasonic guided wave technology may be suitable for this application as it can provide real-time sensing, fast response times, and the ability to reuse the sensor indefinitely. There is the potential for transducers to be kept away from the harsh conditions of the turbine by transmitting a wave through the structure of a blade or vane and analysing the received signal. Measuring temperature in this way reduces the influence of the sensor on the operating condition of the component. The small footprint of the sensors would not affect the operation of components or disrupt airflow. Advancements in sensor materials for use at high temperatures as well as the associated signal processing may allow for sensors to be installed in harsh environments. The following section considers the suitability of acoustic methods for the temperature monitoring of turbine blades and NGVs.

3.1 Ultrasonic Structural Health Monitoring

Ultrasound is of particular interest for SHM applications as it allows for small sensors, high precision, fast data rates, and can be utilised at frequencies much higher than environmental noise [75]. Traditional ultrasonic NDE utilises A-scans, a measurement of signal amplitude against time, to detect cracks, defects etc. This can be extended to B [76], C [77, 78], or phased-array [79] scans to build an image of damage in an area by moving the transducers around and carrying out multiple measurements. This form of evaluation is not particularly suited to turbomachinery applications as the transducers would ideally be permanently installed on the structure. Guided wave SHM is of more interest as constructive interference with surfaces/boundaries allows waves to travel large distances with limited attenuation, which is already utilised for pipe [80] and rail inspection methods [81]. Ultrasound has been proposed as a method of defect detection NDE for aircraft [82], installing transducers in large arrays to allow for guided wave tomography.

When using acoustic waves for SHM and NDE applications either a standalone sensor can be placed in an area of interest, or the structure of interest can directly be used as the sensing medium. In the context of high temperature turbomachinery it would be advantageous to avoid placing sensors into the gas path as they are difficult to interrogate and have the potential to affect operation of the engine components. The structure of turbine blades and NGVs can be used as the sensing medium assuming that an appropriate system of transducers can be implemented.

When considering using a structure as a sensing medium its geometry has an impact on wave propagation. The geometry of a typical turbine blade or NGV is that of a thin plate like structure through which ultrasonic guided waves will propagate. Rayleigh

waves (otherwise known as "Surface Acoustic Waves" (SAWs)) can be excited at high frequencies (at wavelengths much smaller than material thickness) and are confined to the surface of a material, while Lamb waves (otherwise known as "Guided Waves") will propagate if excited at frequencies with wavelengths in the order of material thickness, as they interact with both the top and bottom boundaries of a material. Although Rayleigh waves are non-dispersive they produce large surface motions that are highly sensitive to any discontinuities or defects and are highly affected by surface coatings such as TBCs [83]. Lamb waves will propagate through the multilayered structure of substrate-bonding layer-TBC, where the through-thickness temperature gradient will affect wave propagation, rather than only the temperature at the surface of the TBC.

3.1.1 Temperature Compensation Techniques

In many applications of Lamb wave SHM/NDE the effect of temperature on wave propagation is an undesirable factor that is compensated for using various signal processing techniques. These methods attempt to eliminate the influence of temperature in order to isolate the variable of interest i.e. defects. Temperature compensation or calibration can be carried out by using thermocouples [84], but this is not ideal for the cases where the external use of a sensor is prohibited. Temperature compensation techniques, such as baseline signal stretch (BSS) [85, 86], optimal baseline selection (OBS) [87], hybrid combination of BSS and OBS [88, 89], combination of OBS and adaptive filter algorithm [90], time-of-flight (ToF) calibration based on a linear relationship between the ToF and temperature [91], Hilbert transform and the orthogonal matching pursuit algorithm [92], and temperature compensation for both velocity and phase changes [93, 94] have been proposed to reduce residuals between the baseline signal and the current signal.

BSS method only targets the wave velocity change, neglecting the change in phase and amplitude of the signal. BSS method is restricted for small temperature variations. OBS method can accommodate larger temperature variations, however it requires many baseline signals that have sufficiently low post-subtraction noise levels at different temperatures. Therefore, a combination of BSS and OBS can achieve temperature compensation with a low number of baselines. A new method introduced by Mariani *et al.* [93] considers amplitude and phase changes as well as wave speed changes. It is shown that the residual between the baseline signal and current signals roughly halved when the two signals were acquired at temperatures 15°C apart [93]. Since this method has not been used for measuring the temperature, the sensitivity of the technique has not been analysed.

3.2 Acoustic temperature sensing

Bulk acoustic waves such as longitudinal and shear waves have been used for temperature sensing for a number of years. An overview of temperature sensing using acoustic waves is given by Lynnworth [95]. The most common method of monitoring a change in temperature is to measure a change in acoustic wave time of flight (ToF). This can be calculated from equation 1 [96]:

$$t_F = \frac{d}{v} \tag{1}$$

Where d is the distance travelled at wave speed v , both of which are functions of temperature, T. The sensitivity of the time of flight to temperature can then be expressed as:

$$\delta t_F = \frac{d}{v}\left(\alpha - \frac{k}{v}\right)\delta \mathrm{T} \tag{2}$$

Where α is the coefficient of thermal expansion of the medium and k is the rate of change of wave velocity with temperature:

$$k = \frac{\delta \mathrm{v}}{\delta \mathrm{T}} \tag{3}$$

Monitoring a change in temperature using a change in time of flight provides an average measurement across the transmission path. In the case of turbine blades or nozzle guide vanes there will be a large thermal gradient across the component. Improving spatial resolution may be possible by utilising changes in

time of flight from a number of different reflections, caused by features such as cooling holes or boundaries.

A number of authors have utilised acoustic waves for temperature sensing. Davis *et al.* [97] experimented with an acoustic temperature sensor during variable frequency microwave curing of a polymer-coated silicon wafer. A sapphire buffer rod was used to separate the wafer from a Zinc Oxide (ZnO) transducer centered at approximately 600 MHz. Time of flight (ToF) was measured from the wafer/air interface reflection. Results were comparable to thermocouple measurements from 20°C to 300°C, ±2°C. Takahashi *et al.* [98] carried out 1D measurements of temperature distribution through a 30 mm thick steel plate in contact with molten aluminum (700°C). They noted that the system had a faster response time than the thermocouples used for validation of the method. Jia & Skliar [99, 100] have demonstrated a method for "UltraSound Measurements of Segmental Temperature Distribution" (US-MSTD) in solids, utilising reflections along the signal path to estimate temperature distribution. Three different methods of parametrizing the segmental temperature distribution are discussed. The system has been tested in an oxy-fuel combustor at temperatures up to 1100 degrees, with results comparable to thermocouple measurements [101]. Jeffrey *et al.* [102] demonstrates 2D spatial ultrasonic temperature measurement through a container of wax using 8 0.5 MHz transducers (4 transmitters, 4 receivers), with results comparable to thermocouple measurements. Balasubramaniam *et al.* [103] developed a temperature measurement system in which an externally cooled buffer rod was used to separate an ultrasound transducer from the hot material under test (molten glass). Changes in time of flight (ToF) with temperature were measured from reflections from a notch placed close to the solid-liquid boundary. A calibration procedure carried out from 25°C to 1200°C was used to compensate for the thermal gradients of the delay line, and results were compared against a thermocouple showing a greater than 2% precision. It was noted that the change in ToF due to temperature was greater than the change due to thermal expansion, leading to a non-linear relationship between temperature and time difference. Measurements were then carried out on molten glass with a resolution of 5°C (1 ns precision) using a 10 MHz transducer, however the author suggests resolution could be improved to 0.5°C with faster sampling. Ultrasonic oscillating temperature sensors (UOTSes) are another way to utilise ultrasound for temperature sensing whereby two transducers are setup to transmit through the material of interest in a feedback loop. A number of architectures are desribed by Hashmi *et al.* [104, 105], with sensitivities up to 280 Hz/K [106].

The uses of guided waves for temperature sensing purposes are limited. However, the fundamental antisymmetric Lamb wave mode, A_0, has been used for temperature monitoring of silicon wafers during rapid thermal processing [107, 108]. Quartz pins are used as waveguides, connecting to the wafer through Hertzian contact points. time of flight (ToF) was measured at a rate of 20 Hz from 100°C to 1000°C with an accuracy of ±5°C with this method. A laser excitation system has also been used to measure the temperature of silicon wafers during rapid thermal processing [109]. A broadband excitation pulse is used, and two different methods of signal processing are compared. A cross correlation method between a room temperature baseline signal and those at elevated temperatures, plus a matrix comparison method whereby an unknown signal is compared to a database of signals taken over the whole temperature range of interest. The matrix method was shown to require less signal averaging than the cross-correlation method, with an accuracy in the order of 1°C. The current implementations of acoustic temperature sensors demonstrate the potential of this method, but adapting these systems for use on turbine blades and NGVs will be challenging, starting with the method of effectively coupling to their structure.

3.2.1 Measurement devices for the generation and acquisition of guided waves

The choice of transducer for the generation and acquisition of guided waves is limited by a number of factors including: elevated temperatures, space, and

power consumption.

When transmitting a wave through the structure of a material transducers can either be operated in pulse-echo mode or in a pitch-catch configuration. Pulse-echo mode operates with a single transducer acting as both transmitter and receiver, where the signal reflected from features such as defects or boundaries are analysed. Pitch-catch configurations operate with multiple transducers, some acting as transmitters and some as receivers. Response times are faster in pitch-catch configurations as waves travel directly between transducers rather than requiring a reflection to operate. Systems designed to map defects or damage (tomography) operate in pitch-catch configurations, usually with multiple pairs of transmitters/receivers to allow for higher spatial accuracy. For rotating turbine blades a transducer could be implemented in a pulse-echo configuration, if a transducer could not be housed at the rotating tip of the blade. Transducers could be operated in a pitch-catch configuration on NGVs as transducers could be placed on either side of the static vane.

Piezoelectric based transducers are amongst the most common methods of generating and acquiring acoustic waves. They can be utilised in a number of different ways for either dedicated sensors or for transmitting a wave through a particular structure of interest. Many dedicated sensors are based on the use of interdigital transducers (IDTs) operated as either delay lines or resonators, and are often referred to as surface acoustic wave (SAW) devices. These sensors can be used for high temperature sensing and can be interrogated wirelessly [110, 111], however they would be difficult to implement on the structure of a turbine blade or NGV, while only providing a single point measurement.

In order to transmit a wave through a structure using piezoelectrics there are a number of options, such as wafers and wedges. These sensors are reliant on an effective bond between transducer and substrate, which is difficult to a achieve at high temperatures.

Wedges (Figure 4) can be used to generate surface acoustic waves based on Snell's law [112], where a longitudinal wave produced by a piezoelectric transducer is transmitted through an angled wedge (typically made from a material with a slow longitudinal wave speed relative to the substrate, such as acrylic) into a substrate material where wave refraction takes place. Transmission of shear or surface acoustic waves are dependent on the material properties of the wedge and the substrate, and the wedge angle. A large benefit of this method is the ability to excite single Lamb wave modes in one direction [113]. Unfortunately a liquid couplant is required to form an effective bond between wedge and substrate, which is unlikely to be suitable for permanent installation at high temperatures.

Piezoelectric Wafer Active Sensors (PWAS) are being used extensively for SHM applications and have been shown to withstand exposure to extreme environments [114]. They are non-resonant wide-band devices [115] however they can be used for generation of single Lamb wave modes with careful geometry selection [116]. PWAS are small, inexpensive, and minimally invasive [115], making them potentially suitable for installation on turbine blades and NGVs if a suitable bonding method and piezoelectric material can be found.

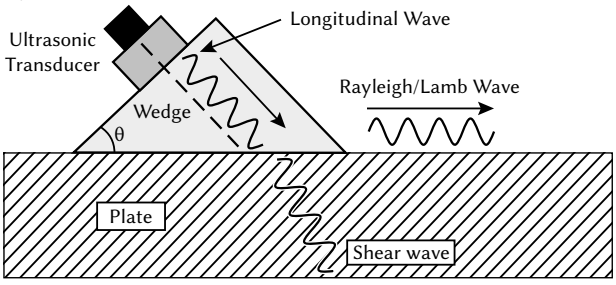

Figure 4: A typical wedge transducer

One promising solution to the bonding problem is to use a waveguide to separate the transducer from the extreme environment of the turbine. This method is especially suited to guided waves as they are known to travel large distances with little attenuation, however the strong reflections from the boundaries of the material can introduce dispersion, and material discontinuities should be considered [117]. One of the main challenges of this method is how to couple the waveguide to the structure of interest, as liquid cou-

plants (as used for wedge coupling) are not suitable for use in high temperature environments, and simple welding is likely to introduce defects causing additional reflections and discontinuities to occur. It has been shown that clamping a waveguide to a structure can be effective even at relatively high temperatures (700°C) [118], although this method may not be suitable for installation on a turbine blade or NGV.

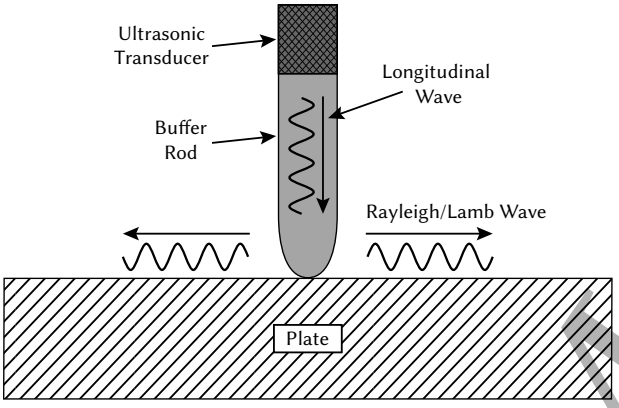

Figure 5: An example hertzian contact transducer

A system of Hertzian contact points (Figure 5) may be more appropriate as only a small point would need to be in contact with the surface of interest. The contact size of the point determines the aperture size of the source, which can be considered as a point source up to very high frequencies, allowing for accurate measurement of absolute velocity [119]. This method of coupling has been used to measure the mechanical properties of carbon fiber reinforced plastics (CFRP) using measured phase velocities of the A_0 and S_0 Lamb wave modes [120]. Application force of the rods can be controlled with springs. An example of a welded waveguide system installed on a turbine vane is given by Willsch [121].

Other options for excitation/acquisition of acoustic waves include electromagnetic acoustic transducers (EMATs)[122] or lasers. Both of these methods could allow for contactless operation, however EMATs are quite inefficient, requiring large amounts of power to produce a signal of adequate amplitude. The use of lasers would require optical access to the surface of interest as well as the installation of a patch to protect the surface of the substrate from laser ablation [123].

Although the use of piezoelectric transducers is likely to be the most appropriate method of exciting acoustic waves for this application, temperature has an effect on their operation [124, 125]. The resonant frequency of a piezoelectric transducer reduces as temperature elevates [124] and if the transducer operates at the resonance ringing may be seen at some temperatures [93]. Filtering methods have been proposed to compensate for the transducer transfer function at different frequencies [126]. Temperature variations affect the bonding stiffness at the interface between the transducer and the structure. This results in frequency response changes which can affect both amplitude and the phase of the signal [127]. A common problem with all methods of excitation using piezoelectrics is their reduction in sensitivity with increasing temperature, which makes the choice of piezoelectric material vitally important.

3.2.2 Piezoelectric selection for high temperature sensing

Piezoelectric materials for high temperature sensors have been compared by a number of authors [128, 129, 130, 117, 131, 132, 133, 134]. Aluminium Nitride (AlN), Langasite (LGS), and Rare Earth Calcium Oxyborate Single Crystals (ReCOB), specifically Yttrium Calcium Oxyborate Single Crystals (YCOB), can be used for high temperature sensing with piezoelectrics [135]. YCOB has the highest operating temperature besides having a high resistivity at high temperatures. This signifies that YCOB will be able to operate at higher temperature as less heat is dissipated with a lower current. YCOB has relative small degradation in sensitivity with increasing temperatures of up to 1000°C, together with no significant phase change up to temperatures of 1500°C, which makes it ideal for high accuracy temperature measurements [136]. YCOB also has a linearly decreasing resistance with temperature, and a close to linearly decreasing resonance frequency with temperature, which can both be used for temperature measurement [137].

Aluminium Nitride (AlN) also exhibits a number of very promising properties necessary for high temperature sensing such as high electrical resistivity, temperature independence of electromechanical properties, and high thermal resistivity of the elastic, dielectric, and piezoelectric properties [138]. The use of an AlN sensor up to 800°C has been demonstrated for detection of laser generated Lamb waves in thin steel plates by Kim [139]. Unfortunately high-quality AlN single crystals are difficult to grow, showing a wide range of resistivity that greatly affects their suitability as ultrasound transducers [140].

It should be noted that although there are a number of piezoelectric materials suitable for use at high temperatures their response would be severely affected by the hot gas flow if installed onto the surface of a blade or vane. Transducers could instead be installed onto the end wall, outside of the main gas path.

3.3 Lamb waves for temperature sensing

The geometry of turbine blades and nozzle guide vanes allows Lamb waves to propagate through their structure at ultrasound frequencies. Lamb waves are a type of elastic wave present in thin plates when wavelength is in the order of thickness. They are guided by the upper and lower boundaries of a material allowing for continuous wave propagation (Figure 6)[141]. A typical nozzle guide vane is thicker (∼3 mm) on the leading edge where it is exposed to the highest temperatures and gas pressures, tapering down to the trailing edge (∼1 mm). This thickness range allows for the excitation of Lamb waves assuming careful frequency selection, which can be determined by analysing dispersion curves generated using material properties. An example of this for Inconel 718 can be found in figure 10.

The bulk acoustic waves discussed previously are non-dispersive, i.e their wave velocities are constant with frequency, whereas Lamb waves are dispersive and multi-modal which makes their analysis complex, especially when their are other factors such as changing temperatures are involved. The lowest order modes, the fundamental antisymmetric mode A_0, and the fundamental symmetric mode S_0 (Figure 9), are the most commonly used modes as they are relatively non-dispersive and comparatively easy to generate in comparison to the higher order modes (A_1, S_1, etc.). Lower order Lamb waves are used extensively for NDE and SHM applications and an overview of their uses for damage identification is provided by Su [142]. Lamb waves have both phase and group velocities, the phase velocity relating to the local speed with which phase of the wave changes, and a group velocity which describes the overall speed of energy transport through the propagating wave. Phase velocity is generally higher than the group velocity. time of flight (ToF) measurements of Lamb waves give the group velocity, while special phase comparison techniques are needed to measure the phase velocity [143].

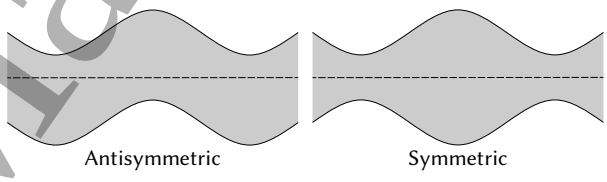

Figure 6: Particle displacement of symmetric and antisymmetric Lamb wave modes in a plate.

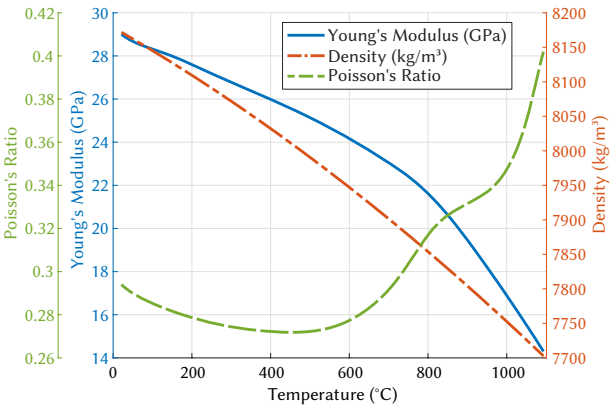

Figure 7: Temperature dependent Young's modulus, density, and calculated Poisson's ratio for Inconel 718.

Lamb waves are affected by three main factors due to changes in temperature: thermal expansion, variations in Young's modulus, and transducer response (including bonding). The effect of temperature on density, Poisson's ratio, and Young's modulus, is shown in Figure 7 for the superalloy Inconel 718 [144, 145]. Nickel based superalloys such as these are commonly used for aerospace components that are exposed to high temperatures. A change in temperature has the greatest relative effect on Young's modulus in comparison to changes in thermal expansion (density and Poisson's ratio)[146]. These changes affect guided wave velocity [147], an example of which is given in figure 8 for the S_0 mode when excited in an aluminium plate using wedge transducers with a 5 cycle tone burst, where it can be seen that an increase in temperature from 20°C to 60°C reduces wave velocity and signal amplitude. A number of authors have investigated the temperature dependence of Lamb waves [148, 149, 96, 146, 150] however their studies are limited to relatively low temperatures.

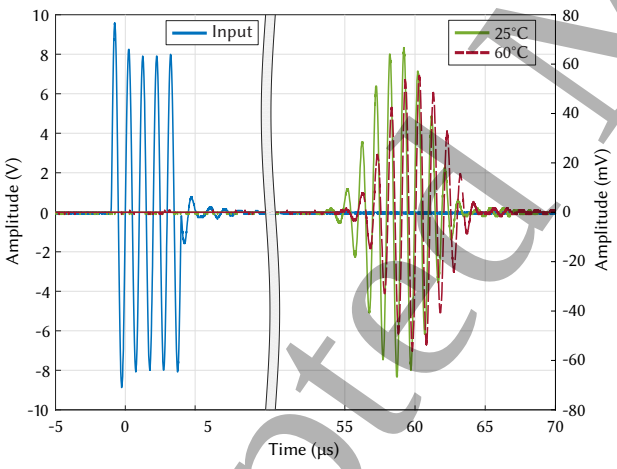

Figure 8: The effect of temperature on the S_0 mode in an aluminium plate.

To better understand the uses of Lamb waves their frequency spectrum can be split into three areas:

- Low frequency region – Contains the lowest two Lamb wave modes (A_0 & S_0). It is possible to selectively excite either mode as they have very different wave velocities, leading to large differences in excitation angle when using a wedge transducer for example.
- Mid-frequency region – Contains many dispersive modes with similar wave speeds making it difficult to excite specific modes without exciting others, leading the production of complex waveforms that are difficult to analyse.
- High frequency region – The modes become less dispersive and converge to similar wave speeds, leading to them travelling as a single packet. Group velocity can be measured for the packet. The A_0 & S_0 modes begin to act like a Rayleigh wave as their velocities converge.

Figure 9 shows phase velocity curves for the symmetric and anti-symmetric Lamb wave modes generated by The Dispersion Calculator [151] for the superalloy Inconel 718. Dispersion curves such as these can be be generated based on material properties allowing areas of interest to be identified.

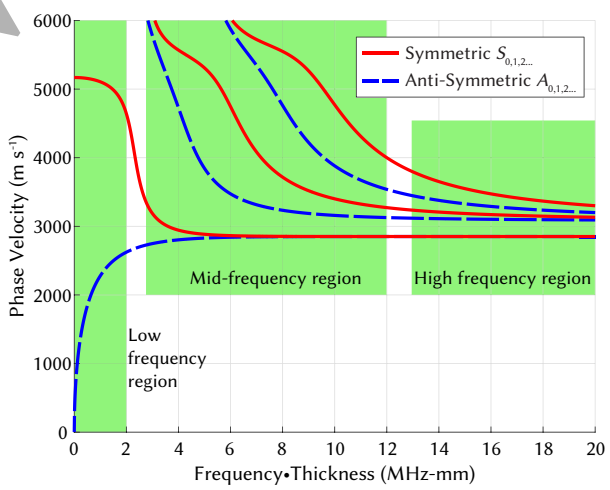

Figure 9: Lamb wave phase velocity dispersion curves for Inconel 718. Modes are displayed in ascending order.

As an example of Lamb wave temperature dependence figure 10 shows the shift in group velocity dispersion curves for the superalloy Inconel 718 from

21°C to 1093°C. An increase in temperature causes a reduction in wave velocity (shifting down) and a reduction along the frequency-thickness axis (shifting left). Temperature sensitivity of the wave velocity varies depending on mode and the dispersiveness of the region excited. Careful selection of excitation frequency can allow for higher temperature sensitivity. As an example figure 11 shows the temperature dependence of the A_0 & S_0 modes at a frequency-thickness product of 1 MHz-mm. The change in wave velocity at this frequency-thickness product is non-linear because of two factors, a non-linear change in Young's modulus with increasing temperature, and the chosen frequency of 1 MHz falling into a more dispersive region as temperature increases, particularly for the S_0 mode. Average temperature sensitivity for the A_0 mode is -0.898 m s^{-1}°C^{-1} and -1.868 m s^{-1}°C^{-1} for the S_0 mode. It can be seen from Figure 10 that the A_0 mode has a relatively linear reduction in wave velocity with increasing temperature regardless of frequency, whereas the other modes have highly dispersive regions (steep slopes) that reduce in frequency (shift to the left) with increasing temperature. Although the wave velocities have a relatively modest temperature sensitivity regardless of mode, a high temperature resolution can be achieved with high precision of velocity measurement. Precision is dependent on sampling frequency and the choice of time of flight (ToF) measurement method [152, 153]. If a sampling rate of 2.5 GHz is used on the example given above over a distance of 10 mm (rough distance to first line of cooling holes) a theoretical velocity resolution of 0.4 m s^{-1} for the S_0 mode and 0.2 m s^{-1} for the A_0 mode can be achieved at 1093°C, which would allow for a temperature resolution of <1°C at 1 MHz. This would require measurements of ToF at sub-wavelength resolution which, although challenging, can be achieved with cross-correlation methods [154, 155]. Linear interpolation of cross-correlation methods can be used to increase resolution without increasing sampling rate [156].

Although the non-dispersive nature of lower order modes (A_0 & S_0) makes them relatively easy to analyse, it would be advantageous to operate at higher frequencies as phase shifts are easier to de-

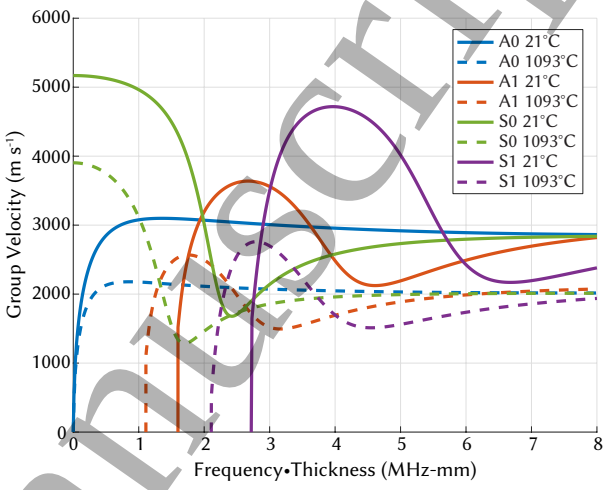

Figure 10: A_0, S_0, A_1, and S_1 group velocity dispersion curve shift with temperature from 21°C to 1093°C for Inconel 718.

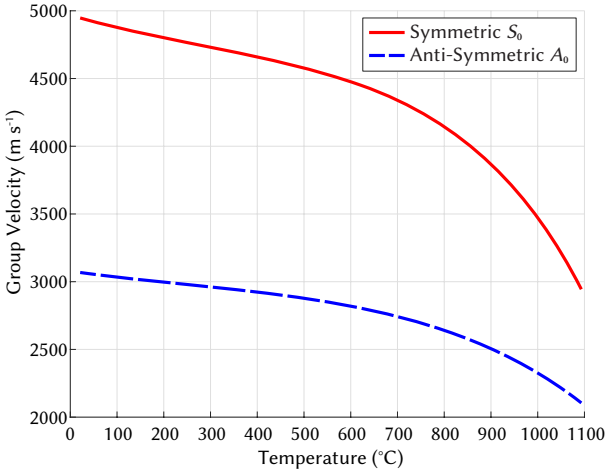

Figure 11: A_0 & S_0 group velocity change with temperature from 21°C to 1093°C at 1 MHz for Inconel 718.

tect when wavelengths are shorter, which leads to improved sensing resolution and accuracy. As the wave speeds of the A_0 & S_0 modes converge (around 10 MHz-mm for Inconel 718) they behave as a Rayleigh wave, which limits their use for this application as discussed previously. Higher order modes such as A_1 & S_1 are more difficult to selectively excite as their phase/group velocities are similar, which leads to the formation of complex waveforms that are highly dispersive. However, as frequency-thickness product is increased further the excitability of higher order modes reduces dramatically which can allow less dispersive regions of lower order modes to be excited [157] (see high frequency region of figure 9). Wilcox *et al.* [158] have presented a method of reducing the effect of dispersion on a transmitted signal if prior knowledge of dispersion curves are known. This relaxes the need to excite only a single mode and simplifies the analysis process. In the case of turbine blades and NGVs, the propagation distance is relatively short so effect of dispersion is likely to be low, however a change in temperature will cause different regions of dispersion curves to be excited which will change the shape of a transmitted wave packet.

Jayaraman *et al.* [159] have presented the existence of "Higher Order Mode Cluster Guided Waves" (HOMC-GW), a non-dispersive region found at high frequency-thickness products in which the various modes all have similar group velocities. This causes them to move as a single envelope, which can be treated like a single non-dispersive mode. A number of aspects of HOMCs have been investigated including: their use for pipe inspections [160, 161, 162], their interaction with weld pads [163], and their interaction with notch-like defects in plates [164]. Khalili & Cawley [113] carried out an investigation into exciting singular higher order modes which found that the HOMC described by Jayaraman was likely to be single mode dominating a cluster (A_1 around 20 MHz-mm). The use of this higher order mode cluster for temperature sensing is of particular interest for turbine blade applications and further investigation is required.

4 Conclusion

A review of the current methods of temperature sensing for turbine blades and NGVs in jet engines has been carried out. Offline systems such as thermal paints and thermal history sensors are well established, but provide limited data in comparison to online systems. When used for the validation of thermal models online systems can provide considerably more information, covering temperature changes through start-up to shut-down of an engine, as well as recording over shoot events. There are a number of online systems available including thin film thermocouples (TFTCs), thermographic phosphors, and pyrometers. Thermocouples need to be embedded into the structure of a component and require a wire connection which is a significant point of failure, while only providing point measurements unless installed in dense arrays. Pyrometers can provide temperature maps without installing sensors onto the surface of a component, but optical access is required, and environmental factors have a significant impact on their accuracy unless specialized long wavelength pyrometers are used. Thermographic phosphors require optical access to components for both excitation and analysis, as well as direct application of a phosphor to the surface. This makes sensors difficult to implement for condition monitoring applications because of space constraints, especially in jet engines.

The ideal sensor for this application would operate outside of the gas path without interfering with operation of components, while still providing a high degree of accuracy with fast response times. Acoustic methods offer a potential advantage in their low power operation and small footprint. Further investigation is required to fully understand wave propagation through the complex geometries of turbine blades and NGVs. This includes coating materials and thicknesses, their temperature dependency, and their degradation (for example pitting and surface microcracking). Changes in surface characteristics can significantly alter the attenuation of guided waves and cracks/defects would cause additional reflections to occur. Residual stresses relating to high temperature gradients will also modify guided wave behaviour

locally. Further investigation is required to determine the best method of attaching transducers to a blade or vane. Using waveguides to reduce the impact of temperature on the operation of transducers is likely to be the most appropriate option for attaching transducers to a vane although there are a number of piezoelectric materials (most notably YCOB and AlN) that would be suitable for use at extremely high temperatures, allowing transducers to be mounted directly onto the end wall of the vane housing. Attaching transducers to rotating turbine blades is likely to be considerably more challenging.

The literature covering the temperature dependence of guided waves is limited to relatively low temperatures and generally only considers the lowest order fundamental Lamb wave modes (A_0 & S_0). To achieve a temperature resolution that is comparable with traditional sensors the frequency of operation needs to be high in order to accurately detect a phase shift with changing temperature, which highlights the potential of higher order modes. Relative measurement of wave velocity is the most common method of temperature sensing using acoustic waves as in most cases (using non-dispersive waves) the change with temperature is linear. When utilising Lamb waves for this purpose careful excitation of single modes will reduce the complexity in signal analysis however this may not be possible with the limited range of transducers and mounting points available. Comparisons with baseline signals may be more appropriate which are already utilised in a number of different temperature compensation techniques. In order to map temperature distribution across a blade the complex series of reflections from cooling holes and boundaries need to be utilised. Reflections can cause mode conversion to take place that has the potential to add additional complexity to the system. This presents a signal processing challenge that has not been previously considered for this application. Further research is planned to evaluate the potential of a guided wave based temperature sensing system for turbine blades and NGVs. The temperature dependence of Lamb wave modes will be theoretically predicted and measured experimentally up to high temperatures. The results of this investigation can be used to determine the most suitable mode for temperature sensing. The interaction between guided waves and cooling holes will be investigated for the purposes of mapping the temperature across a vane. Methods of coupling transducers to the structure of a vane will be considered based on the ability to excite the mode of interest and survive in the high temperature environment of a gas turbine.

References

[1] Federal Aviation Administrator. "Aviation emissions, impacts and mitigation: A primer". In: *Office of Environment and Energy* (2015).

[2] X. Zhang, X. Chen, and J. Wang. "A number-based inventory of size-resolved black carbon particle emissions by global civil aviation". In: *Nature communications* 10.1 (2019), p. 534.

[3] Bahareh Zaghari et al. "High temperature self-powered sensing system for a smart bearing in an aircraft jet engine". In: *IEEE Trans. Instrum. Meas.* (Feb. 2020), pp. 1–1. ISSN: 0018-9456. DOI: 10.1109/tim.2020.2971288.

[4] Bahareh Zaghari et al. "Integrated smart bearings for next generation aero-engines. Part II: Energy harvesting and wireless communication Development". In: *WCCM 2017 - 1st World Congr. Cond. Monit. 2017* (2017).

[5] Clive Kerr and Paul Ivey. "An overview of the measurement errors associated with gas turbine aeroengine pyrometer systems". In: *Meas. Sci. Technol.* 13.6 (2002), pp. 873–881. ISSN: 09570233. DOI: 10.1088/0957-0233/13/6/307.

[6] William J. Becker et al. "Dynamic turbine blade temperature measurements". In: *J. Propuls. Power* 10.1 (1994), pp. 69–78. ISSN: 07484658. DOI: 10.2514/3.23713.

[7] Wenwu Zhou. "Novel cooling strategies for improved protection of gas turbine blades". In: *Grad. Theses Diss.* (2016). URL: https://lib.dr.iastate.edu/etd/15167.

[8] S. L. Dixon and C. A. Hall. *Fluid mechanics and thermodynamics of turbomachinery, 7th edition*. Elsevier, 2013, pp. 1–537. ISBN: 9780124159549. DOI: 10.1016/C2011-0-05059-7.

[9] A. L. Heyes. *Thermographic Phosphor thermometry for gas turbines*. Von Karmen Institute for fluid dynamics, 2004.

[10] Jayant Gopal Thakare et al. "Thermal barrier coatings - A state of the art review". In: *Met. Mater. Int.* 1.March (2020). ISSN: 20054149. DOI: 10.1007/s12540-020-00705-w. URL: https://doi.org/10.1007/s12540-020-00705-w.

[11] J. P. Feist. "Development of phosphor thermometry for gas turbines". PhD thesis. University of London, 2001.

[12] Ahmed M. Abdelrhman et al. "Condition monitoring of blade in turbomachinery: A review". In: *Adv. Mech. Eng.* 2014 (2014). ISSN: 16878140. DOI: 10.1155/2014/210717.

[13] Frank Mevissen and Michele Meo. "A review of NDT/structural health monitoring techniques for hot gas components in gas turbines". In: *Sensors (Switzerland)* 19.3 (2019). ISSN: 14248220. DOI: 10.3390/s19030711.

[14] Fahed Abou Nada et al. "Remote temperature sensing on and beneath atmospheric plasma sprayed thermal barrier coatings using thermographic phosphors". In: *Surf. Coatings Technol.* 302 (2016), pp. 359–367. ISSN: 02578972. DOI: 10.1016/j.surfcoat.2016.06.038. URL: http://dx.doi.org/10.1016/j.surfcoat.2016.06.038.

[15] Bahareh Zaghari, Alex Weddell, and Neil White. "Opportunities and challenges for energy harvesting sensor systems for harsh environments". In: *ENSsys 2017 - Proc. 5th Int. Work. Energy Harvest. Energy-Neutral Sens. Syst. Part SenSys 2017*. New York, New York, USA: Association for Computing Machinery, Inc, Nov. 2017, pp. 40–42. ISBN: 9781450354776. DOI: 10.1145/3142992.3143001. URL: http://dl.acm.org/citation.cfm?doid=3142992.3143001.

[16] P. Guan, Y. Ai, and C. Fei. "An Enhanced Flow-Thermo-Structural Modeling and Validation for the Integrated Analysis of a Film Cooling Nozzle Guide Vane". In: *Energies* 12.14 (2019), p. 2775.

[17] E. Findeisen et al. "Evaluation of numerical methods to predict temperature distributions of an experimentally investigated convection-cooled gas-Turbine blade". In: *Proc. ASME Turbo Expo* 5B-2017 (2017), pp. 1–13. DOI: 10.1115/GT2017-64205.

[18] David Peral et al. "Reliable temperature measurement with thermal history paints: An uncertainty estimation model". In: *Proc. ASME Turbo Expo*. Vol. 6. American Society of Mechanical Engineers (ASME), Nov. 2019, p. 10. ISBN: 9780791858677. DOI: 10.1115/GT2019-92087.

[19] Li Yang and Zhi Min Li. "The research of temperature indicating paints and its application in aero-engine temperature measurement". In: *Procedia Eng.* 99 (2015), pp. 1152–1157. ISSN: 18777058. DOI: 10.1016/j.proeng.2014.12.697. URL: http://dx.doi.org/10.1016/j.proeng.2014.12.697.

[20] Neely and Tracy. "Transient response of thermal paints for use on short-duration hypersonic flight tests". In: *14th AIAA/AHI Sp. Planes Hypersonic Syst. Technol. Conf.* (2006), pp. 1–15.

[21] C. Lempereur, R. Andral, and J. Y. Prudhomme. "Surface temperature measurement on engine components by means of irreversible thermal coatings". In: *Meas. Sci. Technol.* 19.10 (2008). ISSN: 13616501. DOI: 10.1088/0957-0233/19/10/105501.

[22] J. Coleto et al. "Phase change materials and thermosensitive painting: Application on smart thermal protection systems". In: *AIAA 57th Int. Astronaut. Congr. IAC 2006* 8 (2006), pp. 5276–5287. DOI: 10.2514/6.iac-06-c2.5.03.

[23] Andrew J Neely. "Thermal paints for hypersonic flight-test". PhD thesis. University of New South Wales, 2010, p. 48.

[24] C Bird et al. "Surface temperature measurements in turbines". In: *AGARD Conf. Proc. 598*. 1998, p. 21.

[25] European Parliament. *Regulation (EC) No 1907/2006 - Registration, Evaluation, Authorisation and Restriction of Chemicals (REACH) - Safety and health at work - EU-OSHA*. 2006. (Visited on 05/07/2020).

[26] Feist, Nicholls, and Heyes. *(12) Patent Application Publication (10) Pub. No.: US 2011/0069735 A1*. 2011.

[27] S. Karmakar Biswas et al. "Thermal history paints - principles and progress". In: *IET Conf. Publ.* 2014.630 CP (2014), pp. 2–7. DOI: 10.1049/cp.2014.0538.

[28] Silvia Araguás Rodríguez et al. "Accelerated thermal profiling of gas turbine components using luminescent thermal history paints". In: *J. Glob. Power Propuls. Soc.* 2 (2018), S3KTGK. ISSN: 2515-3080. DOI: 10.22261/jgpps.s3ktgk.

[29] C. C. Pilgrim et al. "Surface temperature measurements in an industrial gas turbine using thermal history paints". In: *12th Eur. Conf. Turbomach. Fluid Dyn. Thermodyn. ETC 2017* (2017), pp. 1–13. ISSN: 24104833. DOI: 10.29008/etc2017-303.

[30] A. Rabhiou et al. "Phosphorescent thermal history sensors". In: *Sensors Actuators, A Phys.* 169.1 (2011), pp. 18–26. ISSN: 09244247. DOI: 10.1016/j.sna.2011.04.022. URL: http://dx.doi.org/10.1016/j.sna.2011.04.022.

[31] Stéphane Amiel et al. "On the thermal sensitivity and resolution of a YSZ:Er^{3+}/YSZ:Eu^{3+} fluorescent thermal history sensor". In: *Sensors Actuators, A Phys.* 272 (2018), pp. 42–52. ISSN: 09244247. DOI: 10.1016/j.sna.2018.01.040. URL: http://dx.doi.org/10.1016/j.sna.2018.01.040.

[32] A. L. Heyes et al. "Phosphor based temperature indicating paints". In: *Proc. ASME Turbo Expo* 1 (2012), pp. 927–933. DOI: 10.1115/GT2012-69811.

[33] M Annerfeldt et al. "GTX100 Turbine section measurement using a temperature sensitive crystal technique. A comparison with 3D thermal and aerodynamic analysis". In: *PowerGen Eur.* (2004).

[34] Geoff E. Fair, Ronald J. Kerans, and Triplicane A. Parthasarathy. "Thermal history sensor based on glass-ceramics". In: *Sensors Actuators, A Phys.* 141.2 (2008), pp. 245–255. ISSN: 09244247. DOI: 10.1016/j.sna.2007.08.031.

[35] Kin-Ho Lo, Chan-Hung Shek, and Joseph Lai. "Metallurgical temperature sensors". In: *Recent Patents Mech. Eng.* 1.3 (2012), pp. 225–232. ISSN: 22127976. DOI: 10.2174/2212797610801030225.

[36] Daniel P. Madison et al. "Comparison of piston temperature measurement methods: Templugs versus wireless telemetry with thermocouples". In: *J. Eng. Gas Turbines Power* 135.6 (May 2013). ISSN: 07424795. DOI: 10.1115/1.4023493.

[37] A. Yañez Gonzalez et al. "On-line temperature measurement inside a thermal barrier sensor coating during engine operation". In: *J. Turbomach.* 137.10 (2015), pp. 1–9. ISSN: 15288900. DOI: 10.1115/1.4030260.

[38] Franklin Li Duan et al. "Robust thin-film temperature sensors embedded on nozzle guide vane surface". In: *AIAA J.* (2020), pp. 1–5. DOI: 10.2514/1.J058854.

[39] Kenneth G. Kreider. "Sputtered high temperature thin film thermocouples". In: *J. Vac. Sci. Technol. A Vacuum, Surfaces, Film.* 11.4 (1993), pp. 1401–1405. ISSN: 0734-2101. DOI: 10.1116/1.578561.

[40] Dongfang Yang et al. "Laser deposited high temperature thin film sensors for gas turbines". In: *Aircr. Eng. Aerosp. Technol.* 92.1 (2020), pp. 2–7. ISSN: 17488842. DOI: 10.1108/AEAT-11-2018-0292.

[41] Yantao Liu et al. "A highly thermostable In_2O_3/ITO thin film thermocouple prepared via screen printing for high temperature measurements". In: *Sensors (Switzerland)* 18.4 (2018). ISSN: 14248220. DOI: 10.3390/s18040958.

[42] Yanli Zhang et al. "Laser cladding of embedded sensors for thermal barrier coating applications". In: *Coatings* 8.5 (2018), pp. 1–11. ISSN: 20796412. DOI: 10.3390/coatings8050176.

[43] Junchao Gao et al. "Electrical insulation of ceramic thin film on metallic aero-engine blade for high temperature sensor applications". In: *Ceram. Int.* 42.16 (2016), pp. 19269–19275. ISSN: 02728842. DOI: 10.1016/j.ceramint.2016.09.093. URL: http://dx.doi.org/10.1016/j.ceramint.2016.09.093.

[44] T. N. Satish et al. "Functional validation of K-type (NiCr-NiMn) thin film thermocouple on low pressure turbine nozzle guide vane (LPT NGV) of gas turbine engine". In: *Exp. Tech.* 41.2 (2017), pp. 131–138. ISSN: 17471567. DOI: 10.1007/s40799-016-0162-1.

[45] Zhonglin Ji et al. "Temperature distribution measurements on turbine blade surface by the aid of simple dotted Pt/PtRh thermal couple test array". In: *AIAA Propuls. Energy Forum Expo. 2019* 1.August (2019), pp. 10–13. DOI: 10.2514/6.2019-4084.

[46] Jih Fen Lei, Lisa C. Martin, and Herbert A. Will. "Advances in thin film sensor technologies for engine applications". In: *Proc. ASME Turbo Expo* 4 (1997). DOI: 10.1115/97-GT-458.

[47] Erdogan Guk et al. "Performance and durability of thin film thermocouple array on a porous electrode". In: *Sensors (Switzerland)* 16.9 (2016). ISSN: 14248220. DOI: 10.3390/s16091329.

[48] Clive Kerr and Paul Ivey. "Optical pyrometry for gas turbine aeroengines". In: *Sens. Rev.* 24.4 (2004), pp. 378–386. ISSN: 02602288. DOI: 10.1108/02602280410558412.

[49] Dong Li et al. "Turbine blade temperature error as measured with an optical pyrometer under different wavelengths and blade TBC thickness". In: *Appl. Opt.* 58.7 (2019), p. 1626. ISSN: 1559-128X. DOI: 10.1364/ao.58.001626.

[50] Y. B. Yu and W. K. Chow. "Review on an advanced high-temperature measurement technology: The optical fiber thermometry". In: *J. Thermodyn.* 2009 (2009), pp. 1–11. ISSN: 1687-9244. DOI: 10.1155/2009/823482.

[51] Dong Li et al. "Effect of pyrometer type and wavelength selection on temperature measurement errors for turbine blades". In: *Infrared Phys. Technol.* 94.July (2018), pp. 255–262. ISSN: 13504495. DOI: 10.1016/j.infrared.2018.09.004. URL: https://doi.org/10.1016/j.infrared.2018.09.004.

[52] António Araújo. "Multi-spectral pyrometry — a review". In: *Meas. Sci. Technol.* 28 (2017), p. 15.

[53] J. Manara et al. "Long wavelength infrared radiation thermometry for non-contact temperature measurements in gas turbines". In: *Infrared Phys. Technol.* 80 (2017), pp. 120–130. ISSN: 13504495. DOI: 10.1016/j.infrared.2016.11.014. URL: http://dx.doi.org/10.1016/j.infrared.2016.11.014.

[54] Molly M. Gentleman et al. "Noncontact methods for measuring thermal barrier coating temperatures". In: *Int. J. Appl. Ceram. Technol.* 3.2 (2006), pp. 105–112. ISSN: 1546542X. DOI: 10.1111/j.1744-7402.2006.02069.x.

[55] J. R. Markham et al. "Simultaneous short and long wavelength infrared pyrometer measurements in a heavy-duty gas turbine". In: *J. Eng. Gas Turbines Power* 124.3 (2002),

pp. 528–533. ISSN: 07424795. DOI: 10.1115/1.1473822.

[56] James Markham et al. "Aircraft engine-mounted camera system for long wavelength infrared imaging of in-service thermal barrier coated turbine blades". In: *Rev. Sci. Instrum.* 85.12 (2014), pp. 1–8. ISSN: 10897623. DOI: 10.1063/1.4903266.

[57] Stefan L.F. Frank et al. "Application of a high resolution turbine pyrometer to heavy duty gas turbines". In: *Proc. ASME Turbo Expo* 4 (2001). DOI: 10.1115/2001-GT-0577.

[58] Guanghua Wang et al. "Real-time burst signal removal using multicolor pyrometry based filter for improved jet engine control". In: *J. Turbomach.* 137.8 (2015), pp. 1–9. ISSN: 15288900. DOI: 10.1115/1.4029615.

[59] Tomoki Taniguchi et al. "Temperature measurement of high speed rotating turbine blades using a pyrometer". In: *Proc. ASME Turbo Expo* 2 (2006), pp. 521–529. DOI: 10.1115/GT2006-90247.

[60] Stefan Maurer et al. "Design of a Multiple Beam Pyrometer for Measurement of Temperature on Gas Turbine Blades". In: *7th IEEE Conf. Sensors*. i. 2008, pp. 744–747.

[61] M. Willsch et al. "Non Intrusive 8 channel beam pyrometer for gas turbine blade temperature monitoring". In: *7th EVI-GTI Gas Turbine Instrum. Conf. London, 3 - 5 Novemb. 2015*. 2015.

[62] Anders Hellberg. "The siemens SGT-750 gas turbine: Developed for the oil and gas industry". In: *Siemens Ind. Turbomachinary* 1.1 (2018), pp. 1–10.

[63] T Liu and J.P. Sullivan. *Pressure and Temperature Sensitive Paints*. Springer, 2005. ISBN: 3540222413. DOI: 10.1007/b137841.

[64] Mayur D Patel and Mark A Ricklick. "In-house fabrication of temperature sensitive paint for turbine cooling research". In: *Beyond Undergrad. Res. J.* 1.January (2016).

[65] Ashiq Hussain Khalid and Konstantinos Kontis. "Thermographic phosphors for high temperature measurements: Principles, current state of the art and recent applications". In: *Sensors* 8.9 (2008), pp. 5673–5744. ISSN: 14248220. DOI: 10.3390/s8095673.

[66] S. W. Allison and G. T. Gillies. "Remote thermometry with thermographic phosphors: Instrumentation and applications". In: *Rev. Sci. Instrum.* 68.7 (1997), pp. 2615–2650. ISSN: 00346748. DOI: 10.1063/1.1148174.

[67] A. H. Khalid, K. Kontis, and H. Z. Behtash. "Phosphor thermometry in gas turbines: Consideration factors". In: *Proc. Inst. Mech. Eng. Part G J. Aerosp. Eng.* 224.7 (2010), pp. 745–755. ISSN: 09544100. DOI: 10.1243/09544100JAERO560.

[68] Jan Brübach et al. "On surface temperature measurements with thermographic phosphors: A review". In: *Prog. Energy Combust. Sci.* 39.1 (2013), pp. 37–60. ISSN: 03601285. DOI: 10.1016/j.pecs.2012.06.001.

[69] X. Chen et al. "Industrial sensor TBCs: Studies on temperature detection and durability". In: *Int. J. Appl. Ceram. Technol.* 2.5 (2005), pp. 414–421. ISSN: 1546542X. DOI: 10.1111/j.1744-7402.2005.02042.x.

[70] J. P. Feist et al. "Application of an industrial sensor coating system on a rolls-royce jet engine for temperature detection". In: *J. Eng. Gas Turbines Power* 135.1 (2013), pp. 1–9. ISSN: 07424795. DOI: 10.1115/1.4007370.

[71] Thomas P Jenkins et al. "Measurements of turbine blade temperature in an operating aero engine using thermographic phosphors". In: *Meas. Sci. Technol.* 31.4 (2020), p. 044003. ISSN: 0957-0233. DOI: 10.1088/1361-6501/ab4c20.

[72] Jeffrey I. Eldridge. "Luminescence decay-based Y2O3:Er phosphor thermometry: Temperature sensitivity governed by multiphonon emission with an effective phonon energy transition". In: *J. Lumin.* 214 (Aug. 2019),

p. 116535. ISSN: 00222313. DOI: 10.1016/j.jlumin.2019.116535.

[73] Patrick Nau et al. "Wall temperature measurements in gas turbine combustors with thermographic phosphors". In: *J. Eng. Gas Turbines Power* 141.4 (2019), pp. 1–12. ISSN: 15288919. DOI: 10.1115/1.4040716.

[74] Franklin Li Duan et al. "Development of robust high temperature mems sensor on aero-engine turbine blade surface". In: *2018 Jt. Propuls. Conf.* (2018), pp. 1–7. DOI: 10.2514/6.2018-4622.

[75] Mira Mitra and S. Gopalakrishnan. "Guided wave based structural health monitoring: A review". In: *Smart Mater. Struct.* 25.5 (2016). ISSN: 1361665X. DOI: 10.1088/0964-1726/25/5/053001.

[76] M Fatemi. "Ultrasonic B-scan imaging: Theory of image formation and a technique for restoration". In: *Ultrason. Imaging* 2.1 (Jan. 1980), pp. 1–47. ISSN: 01617346. DOI: 10.1016/0161-7346(80)90201-1.

[77] Roman Růžek, Radek Lohonka, and Josef Jironč. "Ultrasonic C-scan and shearography NDI techniques evaluation of impact defects identification". In: *NDT E Int.* 39.2 (Mar. 2006), pp. 132–142. ISSN: 09638695. DOI: 10.1016/j.ndteint.2005.07.012.

[78] K. Imielińska et al. "Air-coupled ultrasonic C-scan technique in impact response testing of carbon fibre and hybrid: Glass, carbon and Kevlar/epoxy composites". In: *J. Mater. Process. Technol.* Vol. 157. SPEC. ISS. Elsevier, Dec. 2004, pp. 513–522. DOI: 10.1016/j.jmatprotec.2004.07.143.

[79] Ichiro Komura, Taiji Hirasawa, and Satoshi Nagai. "Crack detection and sizing technique by ultrasonic and electromagnetic methods". In: *Nucl. Eng. Des.* 206 (2001), pp. 351–362. ISSN: 1068820X. DOI: 10.1007/s11003-011-9382-9.

[80] Bahareh Zaghari, Victor Humphrey, and Mohamed Moshrefi-Torbati. "Dispersion behavior of torsional guided waves in a small diameter steel gas pipe". In: *ICAC 2013 - Proc. 19th Int. Conf. Autom. Comput. Futur. Energy Autom.* 1.September (2013), pp. 37–42.

[81] Hongmei Shi et al. "An ultrasonic guided wave mode selection and excitation method in rail defect detection". In: *Appl. Sci.* 9.6 (2019). ISSN: 20763417. DOI: 10.3390/app9061170.

[82] Yu Wang et al. "A stretchable and large-scale guided wave sensor network for aircraft smart skin of structural health monitoring". In: *Struct. Heal. Monit.* (2019). ISSN: 17413168. DOI: 10.1177/1475921719850641.

[83] K. Dransfeld and E. Salzmann. *Excitation, Detection, and Attenuation of High-Frequency Elastic Surface Waves*. Vol. 7. 1. ACADEMIC PRESS, INC., 1970, pp. 219–272. DOI: 10.1016/B978-0-12-395667-5.50010-6. URL: http://dx.doi.org/10.1016/B978-0-12-395667-5.50010-6.

[84] A. Gajdacsi et al. "Reconstruction of temperature distribution in a steel block using an ultrasonic sensor array". In: *Journal of Nondestructive Evaluation* 33.3 (2014), pp. 458–470.

[85] A. J. Croxford et al. "Strategies for overcoming the effect of temperature on guided wave structural health monitoring". In: *Health Monitoring of Structural and Biological Systems 2007*. Vol. 6532. International Society for Optics and Photonics. 2007, 65321T.

[86] J. B. Harley and J. M. Moura. "Scale transform signal processing for optimal ultrasonic temperature compensation". In: *IEEE transactions on ultrasonics, ferroelectrics, and frequency control* 59.10 (2012), pp. 2226–2236.

[87] G. Konstantinidis, B. W. Drinkwater, and P. D. Wilcox. "The temperature stability of guided wave structural health monitoring systems". In: *Smart Materials and Structures* 15.4 (2006), p. 967.

[88] T. Clarke, F. Simonetti, and P. Cawley. "Guided wave health monitoring of complex structures by sparse array systems: Influence of temperature changes on performance". In: *Journal of Sound and Vibration* 329.12 (2010), pp. 2306–2322.

[89] A. J Croxford et al. "Efficient temperature compensation strategies for guided wave structural health monitoring". In: *Ultrasonics* 50.4-5 (2010), pp. 517–528.

[90] Y. Wang et al. "An adaptive filter–based temperature compensation technique for structural health monitoring". In: *Journal of Intelligent Material Systems and Structures* 25.17 (2014), pp. 2187–2198.

[91] D. Li et al. "A New Approach to Guided Wave Ray Tomography for Temperature-Robust Damage Detection Using Piezoelectric Sensors". In: *Sensors* 18.10 (2018), p. 3518.

[92] G. Liu et al. "Baseline signal reconstruction for temperature compensation in lamb wave-based damage detection". In: *Sensors* 16.8 (2016), p. 1273.

[93] S. Mariani, S. Heinlein, and P. Cawley. "Compensation for temperature-dependent phase and velocity of guided wave signals in baseline subtraction for structural health monitoring". In: *Structural Health Monitoring* (2019), p. 1475921719835155.

[94] B. Herdovics and F. Cegla. "Compensation of phase response changes in ultrasonic transducers caused by temperature variations". In: *Structural Health Monitoring* 18.2 (2019), pp. 508–523.

[95] Lawrence C. Lynnworth and Emmanuel P. Papadakis. *Ultrasonic Measurements for Process Control: Theory, Techniques , Applications*. Vol. 88. 1. Academic Press, Inc., 1990, p. 589. ISBN: 0124605850. DOI: 10.1121/1.399906.

[96] A. J. Croxford et al. "Strategies for guided-wave structural health monitoring". In: *Proc. R. Soc. A Math. Phys. Eng. Sci.* 463.2087 (2007), pp. 2961–2981. ISSN: 14712946. DOI: 10.1098/rspa.2007.0048.

[97] Cleon E. Davis et al. "In situ acoustic temperature measurement during variable-frequency microwave curing". In: *IEEE Trans. Electron. Packag. Manuf.* 31.4 (2008), pp. 273–284. ISSN: 1521334X. DOI: 10.1109/TEPM.2008.2004570.

[98] Manabu Takahashi and Ikuo Ihara. "Ultrasonic determination of temperature distribution in thick plates during single sided heating". In: *Mod. Phys. Lett. B* 22.11 (2008), pp. 971–976. ISSN: 02179849. DOI: 10.1142/S0217984908015693.

[99] Yunlu Jia and Mikhail Skliar. "Non-invasive ultrasound measurements of temperature distribution and heat fluxes in solids". In: *Energy and Fuels* 30.5 (2016), pp. 4363–4371. ISSN: 15205029. DOI: 10.1021/acs.energyfuels.6b00054.

[100] Mikhail Skliar. *In-situ acoustic measurements of temperature profile in extreme environments*. Tech. rep. University of Utah: Department of Energy National Energy Technology Laboratory, 2015.

[101] Yunlu Jia and Mikhail Skliar. "Ultrasonic measurements of temperature distribution and heat fluxes across containments of extreme environments". In: *IEEE Int. Ultrason. Symp. IUS* 2019-Octob (2019), pp. 940–943. ISSN: 19485727. DOI: 10.1109/ULTSYM.2019.8925643.

[102] Taylor Jeffrey, David Jack, and David Moore. "Listening to temperature: Ultrasonic non-destructive identification of material phase and temperature". In: *AIP Conf. Proc.* 2102.May (2019). ISSN: 15517616. DOI: 10.1063/1.5099721.

[103] Krishnan Balasubramaniam et al. "High temperature ultrasonic sensor for the simultaneous measurement of viscosity and temperature of melts". In: *Rev. Sci. Instrum.* 70.12 (1999), pp. 4618–4623. ISSN: 00346748. DOI: 10.1063/1.1150123.

[104] A. Hashmi et al. "Embedded supervisory control and output reporting for the oscillating ultrasonic temperature sensors". In: *Adv. Intell. Syst. Comput.* 348 (2015), pp. 139–150. ISSN: 21945357. DOI: 10.1007/978-3-319-18503-3.

[105] Anas Hashmi and Alexander N. Kalashnikov. "Sensor data fusion for responsive high resolution ultrasonic temperature measurement using piezoelectric transducers". In: *Ultrasonics* 99.July (2019), p. 105969. ISSN: 0041624X. DOI: 10.1016/j.ultras.2019.105969. URL: https://doi.org/10.1016/j.ultras.2019.105969.

[106] Said Alzebda and Alexander N. Kalashnikov. "Ultrasonic sensing of temperature of liquids using inexpensive narrowband piezoelectric transducers". In: *IEEE Trans. Ultrason. Ferroelectr. Freq. Control* 57.12 (2010), pp. 2704–2711. ISSN: 08853010. DOI: 10.1109/TUFFC.2010.1744.

[107] Y. J. Lee, B. T. Khuri-Yakub, and K. C. Saraswat. "Temperature measurement in rapid thermal processing using acoustic techniques". In: *Rev. Sci. Instrum.* 65.4 (1994), pp. 974–976. ISSN: 00346748. DOI: 10.1063/1.1144929.

[108] Y. J. Lee and T Butrus. "Temperature measurement in rapid thermal processing using the acoustic temperature sensor". In: *Solid State Technol.* 40.4 (1997), pp. 63–74. ISSN: 0038111X. DOI: 10.1557/proc-470-3.

[109] Dan Klimek et al. "Laser ultrasonic instrumentation for accurate temperature measurement of silicon wafers in rapid thermal processing systems". In: *Mater. Res. Soc.* 525 (1998), pp. 135–140.

[110] Mauricio Pereira Da Cunha et al. "Recent advances in harsh environment acoustic wave sensors for contemporary applications". In: *Proc. IEEE Sensors* (2011), pp. 614–617. DOI: 10.1109/ICSENS.2011.6126948.

[111] Wenxiu Dong et al. "Sensitivity enhanced temperature sensor: One-port 2D surface phononic crystal resonator based on AlN/sapphire". In: *Semicond. Sci. Technol.* 34.5 (2019). ISSN: 13616641. DOI: 10.1088/1361-6641/ab0a82.

[112] Shuzeng Zhang, Xiongbing Li, and Hyunjo Jeong. "Measurement of Rayleigh wave beams using angle beam wedge transducers as the transmitter and receiver with consideration of beam spreading". In: *Sensors (Switzerland)* 17.6 (2017). ISSN: 14248220. DOI: 10.3390/s17061449.

[113] Pouyan Khalili and Peter Cawley. "Excitation of single mode lamb waves at high frequency thickness products". In: *IEEE Trans. Ultrason. Ferroelectr. Freq. Control* 63.2 (2016), pp. 1–10.

[114] Hanfei Mei et al. "Recent advances in piezoelectric wafer active sensors for structural health monitoring applications". In: *Sensors (Switzerland)* 19.2 (2019). ISSN: 14248220. DOI: 10.3390/s19020383.

[115] Victor Giurgiutiu. "Lamb wave generation with piezoelectric wafer active sensors for structural health monitoring". In: *Smart Struct. Mater. 2003 Smart Struct. Integr. Syst.* 5056.August 2003 (2003), p. 111. ISSN: 0277786X. DOI: 10.1117/12.483492.

[116] Baiyang Ren and Cliff J. Lissenden. "A fully coupled model for actuation of higher order modes of Lamb waves". In: *AIP Conf. Proc.* 1806.February 2017 (2017). ISSN: 15517616. DOI: 10.1063/1.4974577.

[117] David A. Parks, Shujun Zhang, and Bernhard Tittmann. "High-temperature (¿500°C) ultrasonic transducers: An experimental comparison among three candidate piezoelectric materials". In: *IEEE Trans. Ultrason. Ferroelectr. Freq. Control* 60.5 (2013), pp. 1010–1015. ISSN: 08853010. DOI: 10.1109/TUFFC.2013.2659.

[118] Frederic B. Cegla et al. "Monitoring using dry-coupled ultrasonic waveguide transducers". In: *IEEE Trans. Ultrason. Ferroelcetrics Freq. Control* 58.1 (2011), pp. 156–167.

[119] F. Levent Degertekin and Butrus T. Khuri-Yakub. "Lamb wave excitation by hertzian contacts with applications in NDE". In: *IEEE Trans. Ultrason. Ferroelectr. Freq. Control* 44.4 (1997), pp. 769–779. ISSN: 08853010. DOI: 10.1109/58.655191.

[120] Raimond Grimberg et al. "Determination of elastic properties of CFRP using lamb waves resonant spectroscopy". In: *NDT Aerosp.* 1.March 2015 (2010), pp. 5–12.

[121] M. Willsch, T. Bosselmann, and N. M. Theune. "New approaches for the monitoring of gas turbine blades and vanes". In: *Proc. IEEE Sensors* 1 (2004), pp. 20–23. DOI: 10.1109/icsens.2004.1426089.

[122] Pouyan Khalili and Peter Cawley. "Relative ability of wedge-coupled piezoelectric and meander coil EMAT probes to generate single-mode lamb waves". In: *IEEE Trans. Ultrason. Ferroelectr. Freq. Control* 65.4 (2018), pp. 648–656. ISSN: 08853010. DOI: 10.1109/TUFFC.2018.2800296.

[123] Taeyang Kim et al. "Narrow band photoacoustic lamb wave generation for nondestructive testing using candle soot nanoparticle patches". In: *Appl. Phys. Lett.* 115.10 (2019). ISSN: 00036951. DOI: 10.1063/1.5100292.

[124] X. Jiang et al. "High-temperature piezoelectric sensing". In: *Sensors* 14.1 (2014), pp. 144–169.

[125] R. Fachberger et al. "Properties of radio frequency Rayleigh waves on langasite at elevated temperatures". In: *IEEE Ultrasonics Symposium, 2004.* Vol. 2. IEEE. 2004, pp. 1223–1226.

[126] A. M. Hurst et al. "Real-time, advanced electrical filtering for pressure transducer frequency response correction". In: *ASME Turbo Expo 2015: Turbine Technical Conference and Exposition.* American Society of Mechanical Engineers. 2015, V006T05A015–V006T05A015.

[127] S. Ha et al. "Adhesive layer effects on PZT-induced lamb waves at elevated temperatures". In: *Structural Health Monitoring* 9.3 (2010), pp. 247–256.

[128] R. C. Turner et al. "Materials for high temperature acoustic and vibration sensors: A review". In: *Appl. Acoust.* 41.4 (1994), pp. 299–324. ISSN: 0003682X. DOI: 10.1016/0003-682X(94)90091-4.

[129] James F. Tressler, Sedat Alkoy, and Robert E. Newnham. "Piezoelectric sensors and sensor materials". In: *J. Electroceramics* 2.4 (1998), pp. 257–272. ISSN: 13853449. DOI: 10.1023/A:1009926623551.

[130] Bernhard R Tittmann, David A Parks, and Shujun O Zhang. "High temperature piezoelectrics - A comparison". In: *13th Int. Symp. Nondestruct. Characterisation Mater.* 1.May (2013), pp. 20–24.

[131] Xiaoning Jiang et al. "High-temperature piezoelectric sensing". In: *Sensors (Switzerland)* 14.1 (2013), pp. 144–169. ISSN: 14248220. DOI: 10.3390/s140100144.

[132] Mark J Schulz et al. "Piezoelectric materials at elevated temperature". In: *J. Intell. Mater. Syst. Struct.* 14.November (2003). DOI: 10.1177/104538903038577.

[133] Shujun Zhang and Fapeng Yu. "Piezoelectric materials for high temperature sensors". In: *J. Am. Ceram. Soc.* 94.10 (2011), pp. 3153–3170. ISSN: 00027820. DOI: 10.1111/j.1551-2916.2011.04792.x.

[134] Shujun Zhang et al. "Recent developments in piezoelectric crystals". In: *J. Korean Ceram. Soc.* 55.5 (2018), pp. 419–439. ISSN: 12297801. DOI: 10.4191/kcers.2018.55.5.12.

[135] T. Stevenson et al. "Piezoelectric materials for high temperature transducers and actuators". In: *Journal of Materials Science: Materials in Electronics* 26.12 (2015), pp. 9256–9267.

[136] H. Zu, H. Wu, and Q-M Wang. "High-temperature piezoelectric crystals for acoustic wave sensor applications". In: *IEEE transactions on ultrasonics, ferroelectrics, and frequency control* 63.3 (2016), pp. 486–505.

[137] Sh. Zhang et al. "Characterization of piezoelectric single crystal $YCa_4O(BO_3)_3$ for high temperature applications". In: *Applied Physics Letters* 92.20 (2008), p. 202905.

[138] Taeyang Kim et al. "High-temperature electromechanical characterization of AlN single crystals". In: *IEEE Trans. Ultrason. Ferroelectr. Freq. Control* 62.10 (2015), pp. 1880–1887. ISSN: 08853010. DOI: 10.1109/TUFFC.2015.007252.

[139] Taeyang Kim, Jinwook Kim, and Xiaoning Jiang. "AlN ultrasound sensor for photoacoustic lamb wave detection in a higherature environment". In: *IEEE Trans. Ultrason. Ferroelectr. Freq. Control* 65.8 (2018), pp. 1444–1451. ISSN: 08853010. DOI: 10.1109/TUFFC.2018.2839034.

[140] Bernhard Tittmann, David A Parks, and Shujun O Zhang. "High Temperature Piezoelectrics - A Comparison". In: *13th Int. Symp. Nondestruct. Characterisation Mater.* May (2013), pp. 20–24.

[141] Joseph L. Rose. *Ultrasonic guided waves in solid media*. Vol. 9781107048. Cambridge University Press, 2014, pp. 1–512. ISBN: 9781107273610. DOI: 10.1017/CBO9781107273610.

[142] Zhongqing Su and Lin Ye. *Identification of damage using Lamb waves: From fundamentals to applications*. Vol. 48. Springer, 2009. ISBN: 9781848827837. DOI: 10.1007/978-1-84882-784-4.

[143] J. David N. Cheeke. *Fundamentals and applications of ultrasonic waves*. 1st ed. CRC Press, 2000, p. 3. ISBN: 0849301300.

[144] R. N. Abdullaev et al. "Density and volumetric expansion of the Inconel 718 alloy in solid and liquid states". In: *Thermophys. Aeromechanics* 26.5 (2019), pp. 785–788. ISSN: 15318699. DOI: 10.1134/S0869864319050160.

[145] Special Metals. *IN718 Datasheet*. 2007. DOI: SMC-066. URL: https://www.specialmetals.com/assets/smc/documents/inconel_alloy_718.pdf.

[146] Saqlain Abbas et al. "Optimization of ultrasonic guided wave inspection in structural health monitoring based on thermal sensitivity evaluation". In: *J. Low Freq. Noise Vib. Act. Control* (2020). ISSN: 20484046. DOI: 10.1177/1461348419886189.

[147] R. .L Weaver and O. I. Lobkis. "Temperature dependence of diffuse field phase". In: *Ultrasonics* 38.1-8 (2000), pp. 491–494.

[148] J. C. Dodson and D. J. Inman. "Thermal sensitivity of Lamb waves for structural health monitoring applications". In: *Ultrasonics* 53.3 (2013), pp. 677–685. ISSN: 0041624X. DOI: 10.1016/j.ultras.2012.10.007. URL: http://dx.doi.org/10.1016/j.ultras.2012.10.007.

[149] Alessandro Marzani and Salvatore Salamone. "Numerical prediction and experimental verification of temperature effect on plate waves generated and received by piezoceramic sensors". In: *Mech. Syst. Signal Process.* 30 (2012), pp. 204–217. ISSN: 08883270. DOI: 10.1016/j.ymssp.2011.11.003. URL: http://dx.doi.org/10.1016/j.ymssp.2011.11.003.

[150] Jochen Moll et al. "Temperature affected guided wave propagation in a composite plate complementing the Open Guided Waves Platform". In: *Sci. data* 6.1 (2019), p. 191. ISSN: 20524463. DOI: 10.1038/s41597-019-0208-1.

[151] Armin Huber. *The Dispersion Calculator*. 2020. URL: https://www.dlr.de/zlp/en/desktopdefault.aspx/tabid-14332/24874%7B%5C_%7Dread-61142/%7B%5C#%7D/gallery/33485.

[152] Luis Espinosa et al. "Accuracy on the time-of-flight estimation for ultrasonic waves applied to non-destructive evaluation of standing trees: A comparative experimental study". In: *Acta Acust. united with Acust.* 104.3 (2018), pp. 429–439. ISSN: 18619959. DOI: 10.3813/AAA.919186.

[153] Linas Svilainis. "Review of high resolution time of flight estimation techniques for ultrasonic signals". In: *52nd Annu. Conf. Br. Inst. Non-Destructive Test. 2013, NDT 2013* 1.September 2013 (2013), pp. 231–242.

[154] Lecheng Jia et al. "A high-resolution ultrasonic ranging system using laser sensing and a cross-correlation method". In: *Appl. Sci.* 9.7 (2019). ISSN: 20763417. DOI: 10.3390/app9071483.

[155] Md Omar Khyam et al. "Highly accurate time-of-flight measurement technique based on phase-correlation for ultrasonic ranging". In: *IEEE Sens. J.* 17.2 (2017), pp. 434–443. ISSN: 1530437X. DOI: 10.1109/JSEN.2016.2631244.

[156] José F.S. Costa-Júnior et al. "Measuring uncertainty of ultrasonic longitudinal phase velocity estimation using different time-delay estimation methods based on cross-correlation: Computational simulation and experiments". In: *Meas. J. Int. Meas. Confed.* 122.May 2017 (2018), pp. 45–56. ISSN: 02632241. DOI: 10.1016/j.measurement.2018.01.073. URL: https://doi.org/10.1016/j.measurement.2018.01.073.

[157] P. Wilcox. "Modeling the excitation of lamb and SH waves by point and line sources". In: *AIP Conf. Proc. 700*. Vol. 206. April 2004. 2004, pp. 206–213. ISBN: 073540173X. DOI: 10.1063/1.1711626.

[158] Paul D. Wilcox. "A rapid signal processing technique to remove the effect of dispersion from guided wave signals". In: *IEEE Trans. Ultrason. Ferroelectr. Freq. Control* 50.4 (2003), pp. 419–427. ISSN: 08853010. DOI: 10.1109/TUFFC.2003.1197965.

[159] Chandrasekaran Jayaraman, C. V. Krishnamurthy, and Krishnan Balasubramaniam. "Higher order modes cluster (HOMC) guided waves - A new technique for NDT inspection". In: *AIP Conf. Proc.* 1096 (2009), pp. 121–128. ISSN: 0094243X. DOI: 10.1063/1.3114094.

[160] A A Swaminathan et al. "Higher Order Mode Cluster (HOMC) guided wave testing of corrosion under pipe supports (CUPS)". In: *Proc. Natl. Semin. Exhib. Non-Destructive Eval.* (2011), pp. 224–227.

[161] Jayaraman Chandrasekaran, C. V. Krishnamurthy, and Krishnan Balasubramaniam. "Axial higher order modes cluster (A-HOMC) guided wave for pipe inspection". In: *AIP Conf. Proc.* 1211.2010 (2010), pp. 161–168. ISSN: 0094243X. DOI: 10.1063/1.3362262.

[162] Krishnan Balasubramaniam et al. "Imaging Hidden Corrosion Using Ultrasonic Non- Dispersive Higher Order Guided Wave Modes". In: *AIP Conf. Proc.* Vol. 975. 215. 2008.

[163] Bhupesh Verma, Swaminathan Annamalai, and Prabhu Rajagopal. "The effect of curvature on the scattering of circumferential higher order mode cluster (C-HOMC) from changes in cross-section". In: *Proc. Natl. Semin. Exhib. Non-Destructive Eval.* 2011.

[164] K. Sri Harsha Reddy et al. "Interaction of Higher Order Modes Cluster (HOMC) guided waves with notch-like defects in plates". In: *AIP Conf. Proc.* 1806.February (2017). ISSN: 15517616. DOI: 10.1063/1.4974583.